การเกิด N_2O และ SO_3 บนตัวเร่งปฏิกิริยาโลหะออกไซด์ผสม V-W-Mo/TiO_2 ระหว่างการเกิดรีดักชันแบบเลือกเกิดของ NO ด้วย NH_3

นางสาววีรนุช กุลจรัสปกรณ์

วิทยานิพนธ์นี้เป็นส่วนหนึ่งของการศึกษาตามหลักสูตรปริญญาวิศวกรรมศาสตรมหาบัณฑิต

สาขาวิชาวิศวกรรมเคมี ภาควิชาวิศวกรรมเคมี

คณะวิศวกรรมศาสตร์ จุฬาลงกรณ์มหาวิทยาลัย

ปีการศึกษา 2555

FORMATION OF N_2O AND SO_3 ON MIXED METAL OXIDE V-W-Mo/TiO_2 CATALYST DURING THE SELECTIVE REDUCTION OF NO BY NH_3

Miss Weeranuch Kuljaratpakorn

A Thesis Submitted in Partial Fulfillment of the Requirements
for the Degree of Master of Engineering Program in Chemical Engineering
Department of Chemical Engineering
Faculty of Engineering
Chulalongkorn University
Academic Year 2012

Thesis Title	FORMATION OF N_2O AND SO_3 ON MIXED METAL OXIDE V-W-Mo/TiO_2 CATALYST DURING THE SELECTIVE REDUCTION OF NO BY NH_3
By	Miss Weeranuch Kuljaratpakorn
Field of Study	Chemical Engineering
Thesis Advisor	Associate Professor Tharathon Mongkhonsi, Ph.D.

Accepted by the Faculty of Engineering, Chulalongkorn University in Partial Fulfillment of the Requirements for the Master's Degree

……....Dean of the Faculty of Engineering
(Associate Professor Boonsom Lerdhirunwong, Dr.Ing.)

THESIS COMMITTEE

……Chairman
(Assistant Professor Suphot Phatanasri, Ph.D.)

……Thesis Advisor
(Associate Professor Tharathon Mongkhonsi, Ph.D.)

……Examiner
(Associate Professor Bunjerd Jongsomjit, Ph.D.)

……External Examiner
(Peangpit Wongmaneenil, D.Eng.)

วีรนุช กุลจรัสปกรณ์: การเกิด N_2O และ SO_3 บนตัวเร่งปฏิกิริยาโลหะออกไซด์ผสม V-W-Mo/TiO_2 ระหว่างการเกิดรีดักชันแบบเลือกเกิดของ NO ด้วย NH_3. (FORMATION OF N_2O AND SO_3 ON MIXED METAL OXIDE V-W-Mo/TiO_2 CATALYST DURING THE SELECTIVE REDUCTION OF NO BY NH_3) อ.ที่ปรึกษาวิทยานิพนธ์หลัก: รศ.ดร. ธราธร มงคลศรี, 69 หน้า.

งานวิจัยนี้ศึกษาการเกิด N_2O และ SO_3 บนตัวเร่งปฏิกิริยาโลหะออกไซด์ผสม V-W-Mo/TiO_2 ระหว่างการเกิดรีดักชันแบบเลือกเกิดของ NO ด้วย NH_3 โดยใช้ตัวเร่งปฏิกิริยาของงานวิจัยก่อนหน้า (Piyanantarak, 2011) ซึ่งเตรียม TiO_2 ด้วยวิธี sol-gel ทำการเติมโลหะ V_2O_5, WO_3, MoO_3 ลงบน TiO_2 ด้วยวิธีเคลือบฝังแบบเปียกพอดีรูพรุนและได้ทำการวิเคราะห์ ICP-OES, nitrogen adsorption และ NH_3-TPD ไว้แล้ว แต่ในงานวิจัยนี้ได้ทำการวิเคราะห์ด้วยเทคนิค XRD และ FT-IR เพิ่มเติมเพื่อตรวจสอบสมบัติของตัวเร่งปฏิกิริยาว่ามีการเปลี่ยนแปลงหรือไม่ การทดสอบปฏิกิริยาทำในช่วงอุณหภูมิการทำปฏิกิริยา 120-450 °C พบว่า ในช่วงอุณหภูมิต่ำนั้นจะเกิดกลไกแบบ Eley-Rideal โดยกลไกนี้จะเป็นตัวกำหนดความว่องไวของปฏิกิริยา SCR แต่ในช่วงอุณหภูมิสูงขึ้นปริมาณ NH_3 ที่ดูดซับบนพื้นผิวของตัวเร่งปฏิกิริยาจะเป็นตัวกำหนดความว่องไวของปฏิกิริยา SCR ส่วนการเกิด N_2O นั้นเกิดจากปฏิกิริยาระหว่าง NO และ NH_3 และการออกซิไดซ์ของ NH_3 จะเกิดปฏิกิริยาแบบเอกพันธ์ ระหว่าง NH_3 กับ O_2 และกลไกรีดอกซ์ ส่วนการเกิด SO_3 นั้นตรวจไม่พบพีคของ SO_3

ภาควิชา : วิศวกรรมเคมี ลายมือชื่อนิสิต .....

สาขาวิชา : วิศวกรรมเคมี ลายมือชื่อ อ.ที่ปรึกษาวิทยานิพนธ์หลัก .....

ปีการศึกษา : 2555

5470378521: MAJOR CHEMICAL ENGINEERING
KEYWORDS: FORMATION OF N_2O/ FORMATION OF SO_3/ MIXED METAL OXIDE / SELECTIVE REDUCTION/ TITANIUM (IV) OXIDE

WEERANUCH KULJARATPAKORN: FORMATION OF N_2O AND SO_3 ON MIXED METAL OXIDE V-W-Mo/TiO_2 CATALYST DURING THE SELECTIVE REDUCTION OF NO BY NH_3. ADVISOR: ASSOC.PROF. THARATHON MONGKHONSI, Ph.D., 69 pp.

This research studied the formation of N_2O and SO_3 on mixed metal oxide V-W-Mo/TiO_2 catalyst during the selective reduction of NO by NH_3. This work use a catalyst of previous research (Piyanantarak, 2011) which the TiO_2 support was prepared by sol-gel method and V_2O_5, WO_3, MoO_3 were loaded to TiO_2 support by the incipient wetness method. The catalysts have been already characterized by ICP-OES, nitrogen adsorption and NH_3-TPD. In this study the catalysts are additionally characterized by XRD and FT-IR techniques. The performances of V_2O_5-WO_3-MoO_3/TiO_2 catalyst are measured in the reaction temperature range 120-450 °C. From the results it can be concluded that the SCR process probably occurred from Eley–Rideal mechanism and this mechanism determines the activity of SCR in the low temperature range. However in the high temperature range the amount of adsorbed NH_3 on surface catalysts determines how much NO conversion can be achieved.

The formation of N_2O causes from the reaction between NO and adsorbed NH_3.

The oxidation of NH_3 occurs via homogeneous between NH_3 and O_2 and via redox mechanism. The formation of SO_3 does not occur.

Department : Chemical Engineer Student's Signature .....
Field of Study : Chemical Engineer Advisor's Signature .....
Academic Year : 2012

ACKNOWLEDGEMENTS

I am grateful to all the people who made possible the success of this project and who gave me two wonderful and unforgettable years. My deepest gratitude goes first and foremost to advisor, Assoc. Prof. Tharathon Mongkhonsi. He introduced me to the concept and method about how to make a research, thinking, and experimental techniques. Without his constant instruction for my studies, I could not achieve this work.

I would like to thank my family for supporting me for continually pushes myself to succeed in during these years of my studies.

The financial support from the PTT Public Company Limited is gratefully acknowledged.

CONTENTS

CHAPTER PAGE

LIST OF TABLES

LIST OF FIGURES

FIGURE PAGE

FIGURE PAGE

CHAPTER I

INTRODUCTION

Nitrogen oxides (NO_x) consist of nitric oxide (NO), nitrogen dioxide (NO_2) and nitrous oxide (N_2O). Nitrogen oxides are produced in combustion process of stationary and mobile sources. At high temperatures, oxygen reacts with nitrogen in air to produce nitrogen oxides. Formation of nitrogen oxides are an important problem of air pollution and are greenhouse gases, health effects and can react with water to make nitric acid which result in acid rain.

NO_x emissions from stationary sources (e.g. power plants) can be reduced by incinerator systems process designed and removed NO_x before emitting combustion gases into the atmosphere. There are many techniques for elimination nitrogen oxides. The selective catalytic reduction (SCR) of nitrogen oxides with ammonia in the presence of oxygen is the widely technics for the removal of nitrogen oxide in the stack gases of power plants and of other stationary sources. The SCR process is a process in which a reducing agent, NH_3 reacts selectively with NO_x to produce nitrogen and water according to the two main reactions.

$$4NO + 4NH_3 + O_2 \longrightarrow 4N_2 + 6H_2O \qquad \text{(eq. 1.1)}$$

$$2NO_2 + 4NH_3 + O_2 \longrightarrow 3N_2 + 6H_2O \qquad \text{(eq. 1.2)}$$

NH_3 oxidation is an undesired side reaction at high operating temperature. At high operating temperature NH_3 reacts with oxygen rather than NO to produce nitrogen and nitrogen oxides, according to the reactions.

$$2NH_3 + 3/2O_2 \longrightarrow N_2 + 3H_2O \qquad \text{(eq. 1.3)}$$

$$2NH_3 + 2O_2 \longrightarrow N_2O + 3H_2O \qquad \text{(eq. 1.4)}$$

$$2NH_3 + 5/2O_2 \longrightarrow 2NO + 3H_2O \qquad \text{(eq. 1.5)}$$

In a typical SCR reaction, the catalyst is compounds of vanadium oxide (V_2O_5) coated on various supports such as Al_2O_3 and TiO_2. TiO_2 is used in flue gas

containing SO_2 because TiO_2 resists to SO_2 poisoning in the exhaust gas. Over V_2O_5, SO_2 can be catalytically oxidized to form SO_3. SO_3 can further react with water to form sulfuric acid (H_2SO_4) which is a strong corrosive acid. Moreover, SO_3 can react with ammonia and water to produce ammonium bisulfate and ammonium sulfate which can deposit on the downstream equipment. The reaction mentioned above can be represented by the following equations.

$$2SO_2 + O_2 \longrightarrow 2SO_3 \quad \text{(eq. 1.6)}$$

$$SO_3 + H_2O \longrightarrow H_2SO_4 \quad \text{(eq. 1.7)}$$

$$SO_3 + NH_3 + H_2O \longrightarrow NH_4HSO_4 \quad \text{(eq. 1.8)}$$

$$SO_3 + 2NH_3 + H_2O \longrightarrow (NH_4)_2SO_4 \quad \text{(eq. 1.9)}$$

In order to reduce the SO_2 oxidation, which is another undesired side reaction, it is necessary to reduce the amount of V_2O_5 loading on TiO_2. But reducing of V_2O_5 makes the activity of the catalyst decreases. Therefore, to maintain catalytic activity some metals must be added to the catalyst. Tungsten (W) is a promoter to reduce NH_3 oxidation and improved the catalyst activity at high temperature. The addition of molybdenum (Mo) to the catalyst further increased the activity at low temperature.

A previous work in our research group (Piyanantarak, 2011) presents the NO removal efficiency of the V_2O_5-WO_3-MoO_3/TiO_2 catalysts. That work, however, did not consider the N_2O formation and SO_2 oxidation. The best catalyst in NO removal may not good if too high N_2O and SO_3 occurred during the SCR reaction. The main objectives of this research are to study the N_2O and SO_3 formation in the SCR process of NO by ammonia.

The activity and N_2O formation test of the synthesized catalyst are carried out as a function of reaction temperatures for the SCR. The reaction temperature and the composition of feed are as follows:

Reaction temperature : 120 – 450°C

The composition of feed gas : 120ppm NO, 120ppm NH_3, 30ppmSO_2, 15 vol%O_2, 15vol%H_2O with a balance of N_2.

In the NH_3 oxidation reaction test no NO in the feed stream and NH_3 and H_2O are absence in the SO_2 oxidation test.

This research has been scoped as follows:

1. Additional characterization of catalysts using various techniques to check the properties of the previous work catalysts.

1.1 Determination of the crystal structure by X-ray diffraction technique (XRD).

1.2 Determination of the functional group on the catalyst surface by fourier transform infrared spectroscopy (FTIR).

2. Set up and calibrate a gas chromatograph equipped with an electron capture detector (ECD) for the measurement of NO and N_2O

3. Set up and calibrate a gas chromatograph equipped with a flame photometric detector (FPD) for the measurement of SO_2 and SO_3.

4. Measure the catalytic activity for NO reduction.

5. Measure the N_2O and SO_3 formation in SCR process of NO by NH_3.

6. Measure NO from NH_3 oxidation reaction.

CHAPTER II

THEORY AND LITERATURE REVIEWS

This chapter presents the selective catalytic reduction (SCR) of NO by ammonia, NH_3 oxidation, SO_2 oxidation, V_2O_5-WO_3/TiO_2 and V_2O_5-MoO_3/TiO_2 catalysts and the effect of water in SCR process of NO_x.

2.1 Selective catalytic reduction (SCR) of NO by ammonia

The selective catalytic reduction process is a universally used method for the abatement of NO_x present in waste gas from stationary source (e.g. power plant) due to its efficiency and selectivity. Selective catalytic reduction using NH_3 as reducing agent is selective with NO to produce nitrogen and water. SCR processes are usually carried out in presence of oxygen. Several reactions have been reported to occur during the SCR reaction but it is mostly represented by the following two equations, equations (2.1) and (2.2).

$$4NO + 4NH_3 + O_2 \longrightarrow 4N_2 + 6H_2O \qquad \text{(eq. 2.1)}$$

$$2NO_2 + 4NH_3 + O_2 \longrightarrow 3N_2 + 6H_2O \qquad \text{(eq. 2.2)}$$

Since the concentration of NO_2 in combustion flue gas is relatively low, the dominant reaction is believed to be represented by equation (2.1). More water is produced than nitrogen in each of these reactions.

The ability of ammonia to react selectively with NO_x instead of being oxidized by oxygen is described by the term ‘selective’. Some undesirable reaction can also take place during the SCR of NO with ammonia. These undesired reactions are listed as follows.

$$6NO + 4NH_3 \longrightarrow 5N_2 + 6H_2O \qquad \text{(eq. 2.3)}$$

$$8NO + 2NH_3 \longrightarrow 5N_2O + 3H_2O \qquad \text{(eq. 2.4)}$$

$$4NO + 4NH_3 + 3O_2 \longrightarrow 4N_2O + 6H_2O \qquad \text{(eq. 2.5)}$$

Wong and Nobe (1986) investigated the SCR of nitrogen oxides with ammonia on V_2O_5 and metal oxides supported on TiO_2 and Al_2O_3. It has been reported that Al_2O_3-supported catalysts was less active than TiO_2-supported catalysts. TiO_2-supported produced more N_2O than on Al_2O_3-supported catalysts. In the absence of O_2 according to their experimental results, the order of increasing of catalytic activity was reported as Cr_2O_3/TiO_2 > Fe_2O_3/TiO_2 > V_2O_5/TiO_2 catalysts. In the presence of O_2, the order of increasing of catalytic activity was found to be V_2O_5/TiO_2 > Cr_2O_3/TiO_2 > Fe_2O_3/TiO_2 catalysts. In the presence of O_2, the maximum NO conversion of V_2O_5/TiO_2 catalyst was reported at reaction temperature of 300°C. The maximum NO conversion of Cr_2O_3/TiO_2 catalyst was reported at reaction temperature of 280°C. The maximum NO conversion of Fe_2O_3/TiO_2 catalyst was reported at reaction temperature of 400°C.

2.2 NH_3 oxidation

When the temperature of the SCR reaction increases above about 350°C, NH_3 reacts with oxygen rather than NO to produce nitrogen, nitrogen oxides and nitrous oxide. In the SCR process, the small quantities of nitrous oxide are also produced. N_2O formation is an undesired product during the SCR process.

$$2NH_3 + 3/2O_2 \longrightarrow N_2 + 3H_2O \quad \text{(eq. 2.6)}$$

$$2NH_3 + 2O_2 \longrightarrow N_2O + 3H_2O \quad \text{(eq. 2.7)}$$

$$2NH_3 + 5/2O_2 \longrightarrow 2NO + 3H_2O \quad \text{(eq. 2.8)}$$

Martin et al. (2007) studied the nitrous oxide formation in low operation temperature region during the selective catalytic reduction of nitrogen oxides with V_2O_5/TiO_2 catalysts. This work reported that the high vanadium loading, nitric oxide inlet concentration and reaction temperature increased the formation of nitrous oxide. The mechanism of N_2O generation was proposed based on the interaction of ammonia species adsorbed on bronsted acid sites with nitrate species, which formed by the adsorption of NO + O_2 (finally NO_2) on lewis acid sites. Nitrous oxide was produced by the interaction of two V–ON species on neighboring active site.

2.3 SO_2 oxidation

The sulfur dioxide oxidation represents a highly undesirable side reaction of the selective catalytic reduction of nitrogen oxide since it can provide a very corrosive species. The oxidation of sulfur dioxide to sulfur trioxide follows the reaction

$$2SO_2 + O_2 \longrightarrow 2SO_3 \qquad \text{(eq. 2.9)}$$

Sulfur trioxide presents in flue gases can react with unconverted ammonia and water to form sulfuric acid, ammonium bisulfate (NH_4HSO_4) and ammonium sulfate ($(NH_4)_2SO_4$). These sulfate salts may deposit on the cold equipment downstream of SCR reactor causing plugging, corrosion problems and reduced performances (Svachula et al., 1993)

Catalyst deactivation due to deposition of the ammonium salts was also a problem, if the temperature is not high enough. The ammonium salts can form from the following reactions.

$$SO_3 + H_2O \longrightarrow H_2SO_4 \qquad \text{(eq. 2.10)}$$

$$SO_3 + NH_3 + H_2O \longrightarrow NH_4HSO_4 \qquad \text{(eq. 2.11)}$$

$$SO_3 + 2NH_3 + H_2O \longrightarrow (NH_4)_2SO_4 \qquad \text{(eq. 2.12)}$$

V_2O_5 is the active component in SCR process, the vanadium oxide content is generally kept low in order to reduce sulfur dioxide oxidation (Forzatti et al., 2000)

Amiridis et al. (1996) reported that the presence of SO_2 in the reactant result in the increase in the SCR turnover frequency at low surface vanadia coverage. However, it had no effect at surface vanadia coverage exceeding half a monolayer. The presence of SO_2 resulted in the formation of a surface sulfate species.

Kamata et al. (2001) investigated the effects of V_2O_5 loading of the V_2O_5/TiO_2 SCR catalyst on SO_2 oxidation activity. This work reported that the rate of SO_2 oxidation process increased approximately linearly with V_2O_5 loading under the monolayer capacity.

2.4 V_2O_5-WO_3/TiO_2 and V_2O_5-MoO_3/TiO_2 catalysts

Lietti et al. (1996) studied the reactivity of V_2O_5-WO_3/TiO_2 catalysts in the selective catalytic reduction of nitric oxide by ammonia. They reported that the ternary catalyst presented higher activity in the SCR reaction than the binary V_2O_5/TiO_2 and WO_3/TiO_2 catalysts. The V_2O_5-WO_3/TiO_2 catalyst had a higher surface acidity and higher reducibility than the V_2O_5/TiO_2 catalyst.

The titania support was reported to be very stable, weakly and reversibly sulfated in the presence of SO_2. Vanadium oxide supported on TiO_2-anatase led to very active oxidation catalysts. V_2O_5 was a good dispersion on TiO_2 giving rise to isolated vanadyl centers and polymeric polyvanadate species (Busca et al.,1998)

WO_3 is the promoter which is usually added to increase acidity, activity, the thermal stability of the catalyst and limited the oxidation of SO_2. The addition of MoO_3 to V_2O_5/TiO_2 catalyst improved the resistance toward alkali poisoning.

Nova et al. (1998) studied the characterization and reactivity of TiO_2-supported MoO_3 de-NO_x SCR catalysts. They reported that the activity and selectivity depended on the MoO_3 loading, the activity increased on increasing the MoO_3 content although the selectivity of N_2 decreased due to the N_2O formation. Moreover, they also reported that the MoO_3 addition was not essentially modified the structural and morphological of the TiO_2. The Mo oxide species overspread the strongest TiO_2 acid sites result in the amounts of ammonia adsorbed at high temperature decreased.

Casagrande et al. (1999) investigated the reactivity and redox behavior of V_2O_5-MoO_3/TiO_2 catalysts to compare with the binary V_2O_5/TiO_2 and MoO_3/TiO_2 catalysts having the equal metal oxide loading. They found that the V_2O_5-MoO_3/TiO_2 catalysts were more active than the binary catalysts in SCR reaction at low temperature. They also reported that the ternary catalysts were more easily reduced and reoxidized than the binary catalysts which indicated that the addition of V and Mo improved redox properties. The higher reactivity of V_2O_5-MoO_3/TiO_2 catalysts at low temperature was related to their superior redox properties.

Nova et al. (2001) investigated the thermal deactivation of a commercial de-NO_x V_2O_5-WO_3/TiO_2 catalyst by calcining the catalyst at various temperatures in thetemperature range 500-900°C. They found that the structural and morphological

transitions occur on the starting material increased with increasing temperature of calcination. However, the structural and morphological modifications included the sintering of the TiO_2 support, a decreased of the surface area and the formation of larger pores. At temperature above 850°C, the TiO_2 anatase was transformed to rutile phase. They concluded that the sintering of the TiO_2 support lead to aggregation of isolated vanadium ions, the NH_3 oxidation at high temperature and the undesired SO_2 oxidation.

Pena et al. (2004) studied TiO_2 supported metal oxide (V, Cr, Mn, Fe, Co, Ni and Cu) catalysts for low-temperature selective catalytic reduction of NO with NH_3 in the presence of excess oxygen. They found that the Mn/TiO_2 catalyst was the best performance in SCR of NO by NH_3 at temperature as low as 120°C. The activity of Mn/TiO_2 catalyst increased on increasing the Mn loading and the reaction temperature. The catalytic activity of various metal oxide catalysts was reported to be decreased in the following order: Mn > Cu >> Cr >> Co > Fe >> V >>> Ni. They concluded from NH_3 FTIR studied that the catalysts having lewis acidity were active and that the bronsted acidity did not affect catalytic performance. Moreover, the Mn/TiO_2 catalyst was the best performance when the catalysts were tested in the presence of 11 vol.% H_2O. The catalytic performance of the transition metal oxide supported on TiO_2 decreased in the following order: Mn > V >> Co > Cu > Cr > Fe >> Ni.

Yates et al. (2005) studied the N_2O formation in the SCR process with V_2O_5-WO_3/TiO_2 catalysts. They reported that the mechanisms of nitrous oxide formation depended on the composition of active phase. The undesired compound increased on increasing the vanadia loading in the catalyst. The nitrous oxide was produced by two ammonia molecules were adsorbed over polymeric vanadyl species. Moreover, the nitric oxide molecules adsorbed on nearby centers of the polymeric vanadia to form nitrous oxide in the SCR process.

Lee et al. (2012) investigated the reaction mechanism for the high temperature selective catalytic reduction of NO by NH_3 over a W/TiO_2 catalyst. They reported that the ammonia was first adsorbed and activated at lewis acid sites [W=O] on the surface of the catalyst. Then reacted with NO + O_2 to produce N_2 and H_2O. The lattice oxygen did not affect the catalytic activity although oxygen was involved in

during the redox reaction. At high temperature, the SCR reaction was using ammonia followed the Eley-Rideal mechanism and the SCR process occurred only at W=O sites.

Forzatti et al. (2012) studied the effect of operating variables on the enhanced SCR reaction over a commercial V_2O_5–WO_3/TiO_2 catalyst for stationary applications. They reported that the addition of aqueous solutions of NH_4NO_3 to a NO-NH_3 containing feed stream resulted in the occurrence of an "Enhanced SCR" (E-SCR) reaction ($2NH_3 + 2NO + NH_4NO_3 \longrightarrow 3N_2 + 5H_2O$) over V_2O_5-WO_3/TiO_2 monolith catalyst. They also studied the effects of three main operating variables (temperature, space velocity, ammonium nitrate feed content) in order to identify the best process condition. They found that the best process condition was collected at 180°C with a space velocity of 18 k/h and the feed containing 200 or 250 ppm of NH_4NO_3.

2.5 The effect of water in SCR process of NO_x

Jehng et al. (1996) investigated the effect of water vapor on the molecular structures of V_2O_5 - supported catalysts (SiO_2, Al_2O_3, TiO_2 and CeO_2) by in situ raman spectroscopy as a function of temperature (from 500°C to 120°C). They found that the water had effect on the molecular structures of the surface vanadium oxide species on the $A1_2O_3$, TiO_2 and CeO_2 supports, but no effect on the SiO_2 supports. The raman band of the terminal V=O bond on these oxide supports shifted to lower wavenumbers and became broad upon exposure to moisture. Because of the dehydrated surface VO_x species formed a hydrogen bond with some of the adsorbed moisture. The isolated VO_4 species were dominant at low surface vanadium oxide coverage and the polymeric vanadate species demonstrated that the high surface vanadium oxide coverage. The presence of water vapor decreased NO conversion and increased the selectivity toward N_2O formation at low temperature.

Giakoumelou et al. (2006) investigated the molecular structure and catalytic activity of V_2O_5/TiO_2 catalysts for the SCR reaction. Vanadium oxide was loaded over TiO_2 by wet impregnation method. The SCR reaction was carried out in fixed bed micro reactor. The feed condition was 800 ppm NO, 800 ppm NH_3 and 4% O_2 with N_2 balance. The presence of O_2, NH_3, NO, H_2, H_2O and SO_2 were used in the in

situ raman spectroscopy. The presence of H_2O resulted in the extent of surface hydroxylation, the distribution of bronsted and lewis acid site on the catalyst surface, and the molecular structure of the dispersed surface metal oxides.

2.6 The comment of previous work

From the above review work for the SCR process, it can be concluded that the mostly active phase in reduction of NO_x is V_2O_5. Although V_2O_5 are very active and selective, the undesired oxidation of SO_2 to SO_3 actives if SO_2 presence in feed. (Forzatti et al., 2000)

TiO_2 support is stable and improves the monolayer dispersion of V_2O_5 anatase surface and resistance SO_2.

The additions of WO_3 and MoO_3 to V_2O_5/TiO_2 catalyst improve the catalytic activity, resistance towards alkali poisoning and reduce NH_3 oxidation.

Previous researches usually on the removal of NO_x without considering the occurrence of side reactions and concluded that the catalysts were optimized. However the performance of the catalyst on the side reaction, NH_3 oxidation, SO_2 oxidation and N_2O formation, must be considered due to the catalyst having a high conversion in NO_x reduction may also have N_2O formation and SO_2 oxidation.

Table 2.1 The composition of feed in SCR process.

Authors	**Catalysts**	**Total (ml/min)**	**NO (ppm)**	**NH_3 (ppm)**	**O_2 %v/v**	**H_2O %mol**	**SO_2 (ppm)**	**balance**	**Measure**
Amiridis et al. (1996)	V_2O_5/TiO_2	330	12%	5%	-	-	2%	N_2	NO
Orsenigo et al. (1996)	V_2O_5-WO_3/TiO_2	33	500	550	2	10	500	N_2	NO
Nova et al. (1998)	V_2O_5-MoO_3/TiO_2	120	800	800	9000 (ppm)	-	-	He	NO
Casagrande et al. (1999)	V_2O_5-MoO_3/TiO_2	120	800	800	9000 (ppm)	-	-	He	NO,N_2O
Nova et al. (2001)	V_2O_5-WO_3/TiO_2	120	750	840	2	-	-	He	NO,SO_2
Yates et al. (2005)	V_2O_5-WO_3/TiO_2	-	1000	1000	3	-	-	Ar	NO,N_2O

Authors	**Catalysts**	**Total (ml/min)**	**NO (ppm)**	**NH_3 (ppm)**	**O_2 %v/v**	**H_2O %mol**	**SO_2 (ppm)**	**balance**	**Measure**
Martin et al. (2007)	V_2O_5/TiO_2	-	500/ 1000	1000	3	-	-	N_2	N_2O
Kaewbuddee (2009)	V_2O_5-WO_3/TiO_2	200	120	120	15	15	30	N_2	NO
Taweesuk (2011)	V_2O_5-MoO_3/TiO_2	200	120	120	15	15	30	N_2	NO
Piyanantarak (2011)	V_2O_5-WO_3-MoO_3/TiO_2	200	120	120	15	15	30	N_2	NO,NH_3
Forzatti et al. (2012)	V_2O_5-WO_3/TiO_2	-	500	500	10	10	-	N_2	NO,NH_3
Lee et al. (2012)	WO_3/TiO_2	-	400	420	8	6	-	Ar	NO,NH_3, N_2O

CHAPTER III

EXPERIMENTS

This chapter consists of the catalyst preparation and characterization of catalysts. All catalysts used in the present works were obtained from a previous study (Piyanantarak, 2011). Preparation procedures given here are the procedures carried out in the previous study.

3.1 Catalyst preparation

3.1.1 Chemicals

All chemicals used in this preparation procedure of V_2O_5-WO_3-MoO_3/TiO_2 catalysts are listed in table 3.1.

Table 3.1 The chemicals used in the catalyst preparation.

Chemical	Supplier
Titanium (IV) isopropoxide	Aldrich
Ammonium metavanadate, 99.99%	Aldrich
Ammonium metatungstate hydrate, 99.99%	Aldrich
Ammonium molybdate tetrahydrate, ≥99.0%	Aldrich
Nitric acid 65%	Aldrich
Oxalic acid hydrate	Fluka

3.1.2 Preparation of TiO_2 by sol-gel method

Titanium dioxide was prepared by sol- gel method using the titanium isopropoxide ($Ti(OCH_2CH_2CH_3)_4$) as a precursor. A nitric acid and titanium isopropoxide were carefully added to deionized water and stirred vigorously until a clear solution was obtained. The obtained solution was dialyzed by cellulose membrane until a pH value of 3.5 was reached. The sol-gel was dried at 110°C for 48 hours, crushed and grinded, and finally calcined in a muffle furnace at 350°C for 3 hours.

3.1.3 Preparation of V_2O_5-WO_3-MoO_3 over TiO_2 catalyst

The V_2O_5-WO_3-MoO_3/TiO_2 catalysts were prepared by incipient wetness impregnation methods. The V_2O_5,WO_3 and MoO_3 loadings were selected at 3wt.%, from 3wt.% to 7wt.% and from 3wt.% to 10wt.%, respectively. TiO_2 was used as the support and ammonium metavanadate was used as the precursor for the vanadium oxide. Ammonium metavanadate and oxalic acid were dissolved in deionized water and added to TiO_2 support. The V_2O_5/TiO_2 catalysts were then dried at 120°C for 12 hours in an oven. Ammonium metatungstate hydrate was used as the tungsten precursor. The desired amount of ammonium metatungstate hydrate solution was added to the V_2O_5/TiO_2 catalysts. To obtained V_2O_5-WO_3/TiO_2 catalysts were dried at 120°C for 12 hours. Finally, the amounts of ammonium heptamolybdate which used as the molybdenum precursor was dissolved in deionized water and added to the V_2O_5-WO_3/TiO_2 catalysts, dried in an oven at 120°C for 12 hours and then calcined in air at 500°C for 4 hours.

3.2 Characterization of V_2O_5-WO_3-MoO_3/TiO_2 catalysts

Characterization results of the previous study are summarized here again to help reader not to search back to the previous study.

The prepared V_2O_5-WO_3-MoO_3/TiO_2 catalysts are characterized by nitrogen adsorption to determine the surface area of catalysts, ICP-OES to determine the

amounts of metal loading of catalyst and NH_3-TPD to determine amounts of acid site on the catalyst surface. XRD to analyze crystal structure and the functional group were determined by FT-IR.

3.2.1 BET surface area measurement

BET surface area of TiO_2 and V_2O_5-WO_3-MoO_3/TiO_2 catalysts were measured by nitrogen adsorption at -196°C using Micromeritics ASAP 2020. Prior to analysis, 0.2 g of catalysts was degassed at 200°C for 2 hours under vacuum.

The BET surface area values of the various metal oxides on TiO_2 are compared in table 3.2. The results show that the surface area of all catalysts are lower than TiO_2 support (121.2m^2/g), while the surface area of catalysts decreased as the Mo, WO_3 loading was increased. These values reveal the possibility of a filling effect of the active phase which are plugging or sintering of catalysts.

3.2.2 Inductively Coupled Plasma-Optical Emission Spectroscopy (ICP-OES)

The inductively-coupled plasma optical emission spectroscopy (ICP-OES) Perkin Elmer Optima 2100 DV was used to identify the percentage of metal loading over TiO_2. The catalyst sample approximately 0.02 g. was dissolved in 5 ml hydrofluoric acid 49%, stirred vigorously until the solution became homogeneous and make volume up to 100 ml using de-ionized water by the volumetric flask. The concentration of the sample after volume adjustment is about 1-24 ppm (mg/l). The compositions of the catalysts are shown in table 3.3.

Table 3.2 BET surface areas of the V_2O_5-WO_3-MoO_3/TiO_2 catalysts. (Piyanantarak, 2011)

Catalysts	**Surface area (m^2/g)**	**Pore volume (ml/g)**	**Average pore size (nm)**
TiO_2	121.20	0.2399	7.9140
3V3.5W3Mo	112.13	0.2045	7.2954
3V3.5W5Mo	114.58	0.2007	7.0081
3V3.5W10Mo	108.03	0.1911	7.0769
3V7W3Mo	101.49	0.2003	7.8927
3V7W5Mo	108.78	0.2002	7.3631
3V7W10Mo	101.16	0.1806	7.1430

Table 3.3 The compositions of the V_2O_5-WO_3-MoO_3/TiO_2 catalysts. (Piyanantarak, 2011)

Catalysts	**V_2O_5 (%wt.)**	**WO_3 (%wt.)**	**MoO_3 (%wt.)**
3V3.5W3Mo	3.48	3.59	3.69
3V3.5W5Mo	3.56	3.50	5.44
3V3.5W10Mo	3.79	3.01	11.03
3V7W3Mo	3.71	7.41	3.15
3V7W5Mo	3.03	6.89	5.91
3V7W10Mo	3.44	7.47	11.00

3.2.3 NH_3 Temperature programmed desorption (NH_3-TPD)

Surface acidic property was measured by the NH_3-TPD technique. NH_3-TPD experiments were carried out by the Belcat-A. The amount of NH_3 adsorbed on the surface was determined by thermal conductivity detector. Powdered catalyst samples of 0.05 g. were placed inside quartz tube and preheated through heating in 50 ml/min of pure He from ambient at 10°C/min to 500°C for 1 hour to remove any impurities. After cooling down to 100°C, the catalysts were exposed to a flow of 10vol.% NH_3 in He for 30 minute and then the temperature of the catalysts was raised up to 500°C with a heating rate of 10°C/min in order to allow the desorption of NH_3.

Table 3.4 shows the amount of total acid sites of all catalysts including TiO_2 support, that are calculated from the area under the curve of desorption. Figures 3.1-3.7 show the two peaks in NH_3-TPD profiles. The first obviously peak is found in all figures including TiO_2 support but the second peak is not found in the TiO_2 support profile.

3.2.4 X-Ray Diffraction (XRD)

XRD was used to identify the crystal phases of TiO_2 and V_2O_5-WO_3-MoO_3/TiO_2 catalysts. The catalysts were performed by using D8 Advance of Bruker AXS. CuKα (λ = 0.154056 nm) was used as a radiation source and the spectra were collected in the region of 2θ = 20° - 80° with step size 0.02° and slit width 0.6 nm.

The X-ray diffraction patterns of V_2O_5-WO_3-MoO_3/TiO_2 catalysts of various Mo and W loadings are shown in Figure 3.8. The XRD patterns of all the catalysts appear to contain very sharp peaks at 2θ = 25° and 48° which corresponds to anatase TiO_2 phase and to contain small amounts of rutile and brookite phases. None of the XRD spectra presented give intense or sharp peaks for transition metal oxides (V_2O_5, WO_3 and MoO_3) on the titania support. This may be due to the low crystalline nature (amorphous) or too small crystal size of the metal oxides on the support.

Table 3.4 Amounts of acid site on various V_2O_5-WO_3-MoO_3/TiO_2 catalysts. (Piyanantarak, 2011)

Catalysts	**Amount of total acid site (μmol H^+/g)**	**Temperature of first peak position (°C)**	**Amounts of strong acid site (μmol H^+/g)**	**Temperature of second peak position (°C)**
TiO_2	655	155	-	-
3V3.5W3Mo	476	158	141	405
3V3.5W5Mo	468	150	112	362
3V3.5W10Mo	502	153	103	322
3V7W3Mo	477	162	108	407
3V7W5Mo	491	145	87	360
3V7W10Mo	492	150	89	330

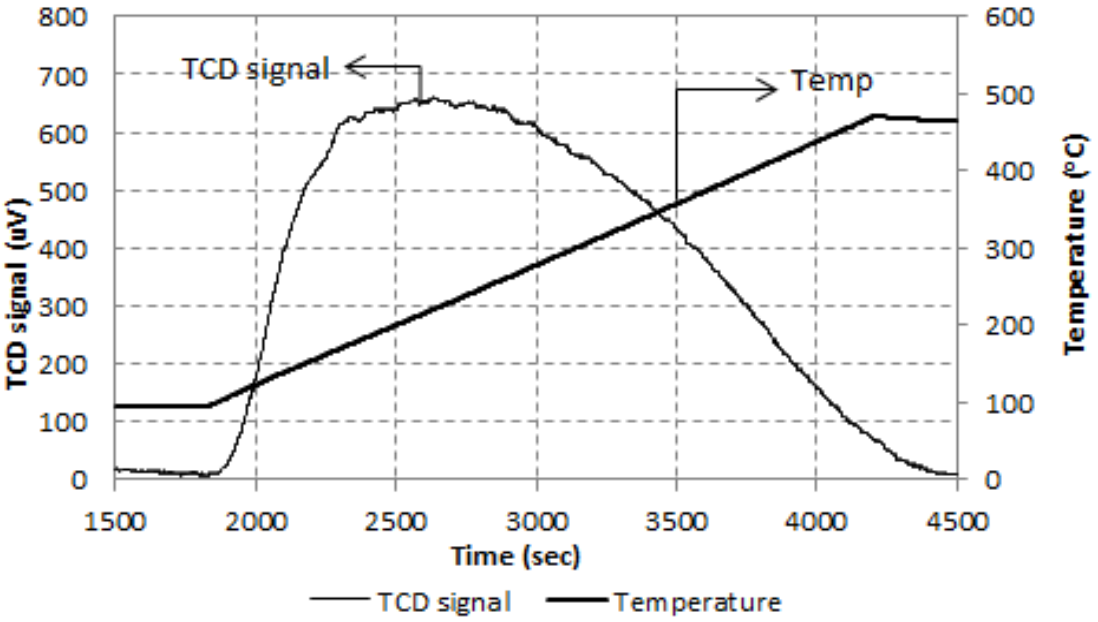

Figure 3.1 NH_3-TPD profiles of TiO_2 support. (Piyanantarak, 2011)

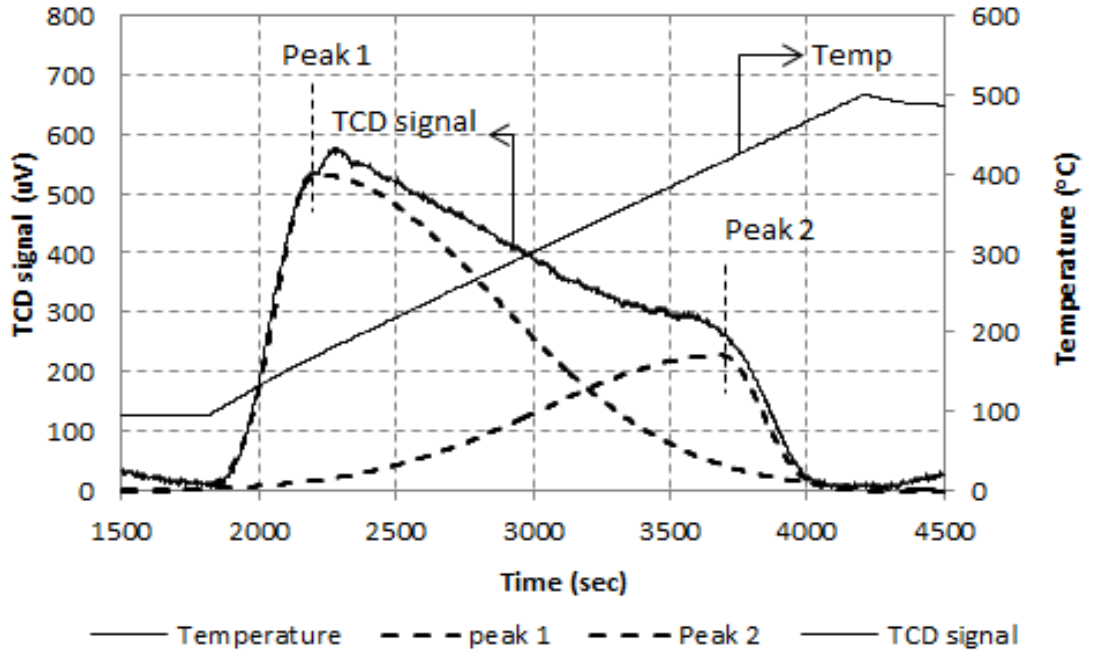

Figure 3.2 NH_3-TPD profiles of 3V3.5W3Mo/TiO_2 catalyst. (Piyanantarak, 2011)

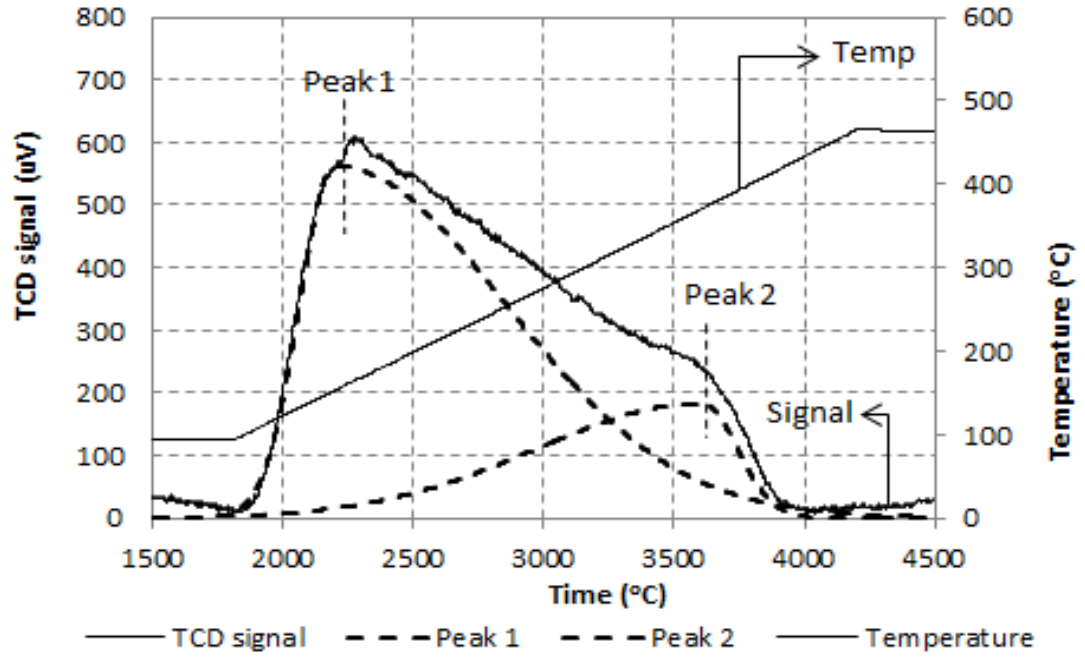

Figure 3.3 NH_3-TPD profiles of 3V3.5W5Mo/TiO_2 catalyst. (Piyanantarak, 2011)

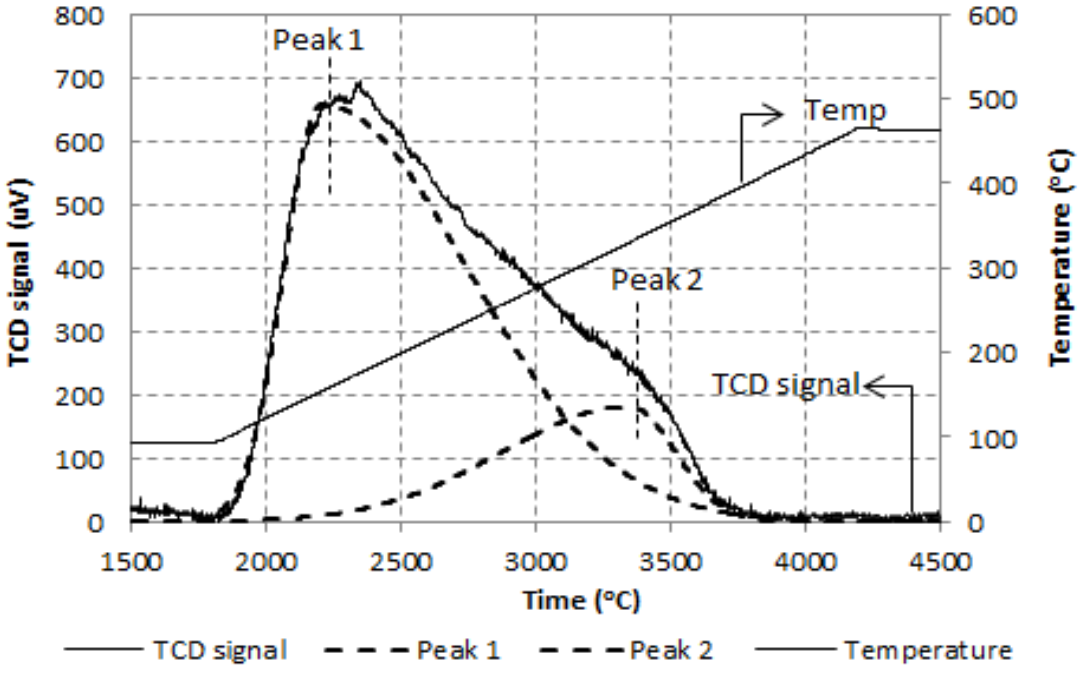

Figure 3.4 NH_3-TPD profiles of 3V3.5W10Mo/TiO_2 catalyst. (Piyanantarak, 2011)

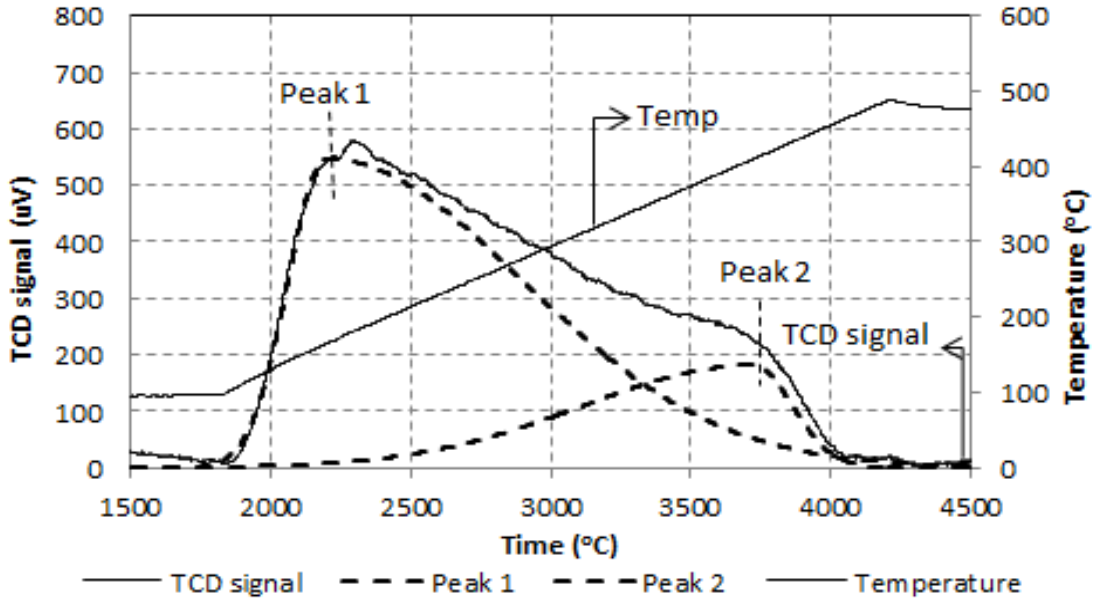

Figure 3.5 NH_3-TPD profiles of 3V7W3Mo/TiO_2 catalyst. (Piyanantarak, 2011)

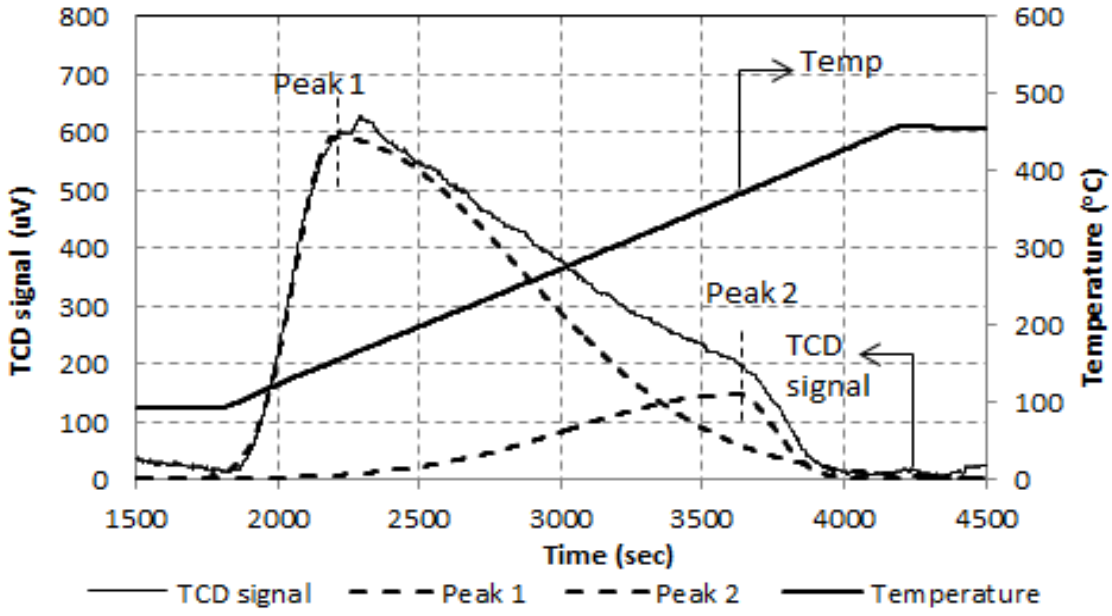

Figure 3.6 NH_3-TPD profiles of 3V7W5Mo/TiO_2 catalyst. (Piyanantarak, 2011)

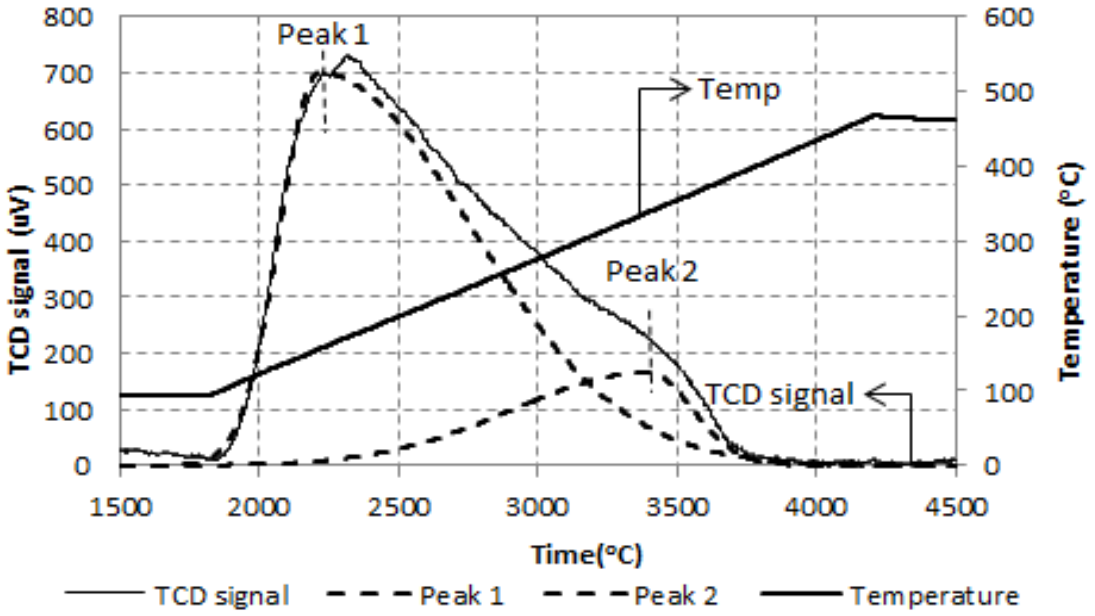

Figure 3.7 NH_3-TPD profiles of 3V7W10Mo/TiO_2 catalyst. (Piyanantarak, 2011)

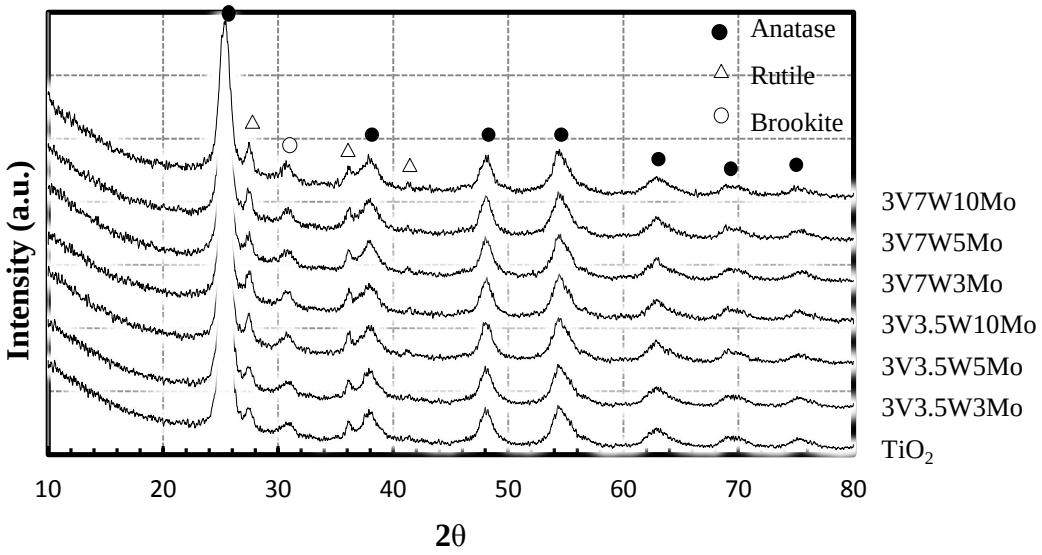

Figure 3.8 XRD patterns of V_2O_5-WO_3-MoO_3/TiO_2 catalysts.

3.2.5 Fourier transforms infrared (FT-IR)

The functional groups on the catalysts surface were determined by FT-IR using nicolet model impact 6700 of the IR spectrometer. The spectra were recorded in the 400 - 4000 cm^{-1} region at each experimental.

The FT-IR spectrum of TiO_2 support is shown in Figure 3.9. The results show strong absorption of TiO_2 anatase in the region 800 – 500 cm^{-1}. The spectrum in the region 3400 – 600 cm^{-1} is C_3H_7O group and the spectrum in the region 3700 – 3400 cm^{-1} and 1725 cm^{-1} is due to the OH stretching band of the surface hydroxyl groups on TiO_2.

The banding of V=O and MoO_3 appeared at wavenumber 1100 – 500 cm^{-1} are shown in Figure 3.10 and Figure 3.12 respectively, but the banding of WO_3 appeared at wavenumber 1000 – 500 cm^{-1} is shown in Figure 3.11.

Figure 3.13 shows FT-IR spectra of the TiO_2 support and the V_2O_5-WO_3-MoO_3/TiO_2 catalysts. The broadening of the band around 970- 930 cm^{-1} was observed at loading of metal oxide (V_2O_5, WO_3 and MoO_3). Also indicates the possible presence of the new oxide of catalysts or low amount of metal oxide.

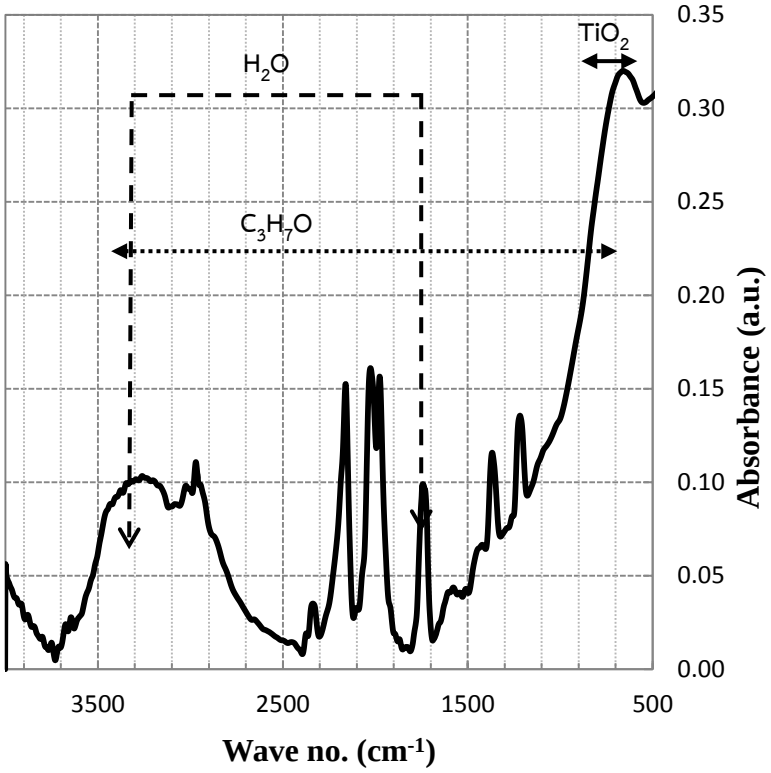

Figure 3.9 FT-IR spectrum of TiO_2. (Piyanantarak, 2011)

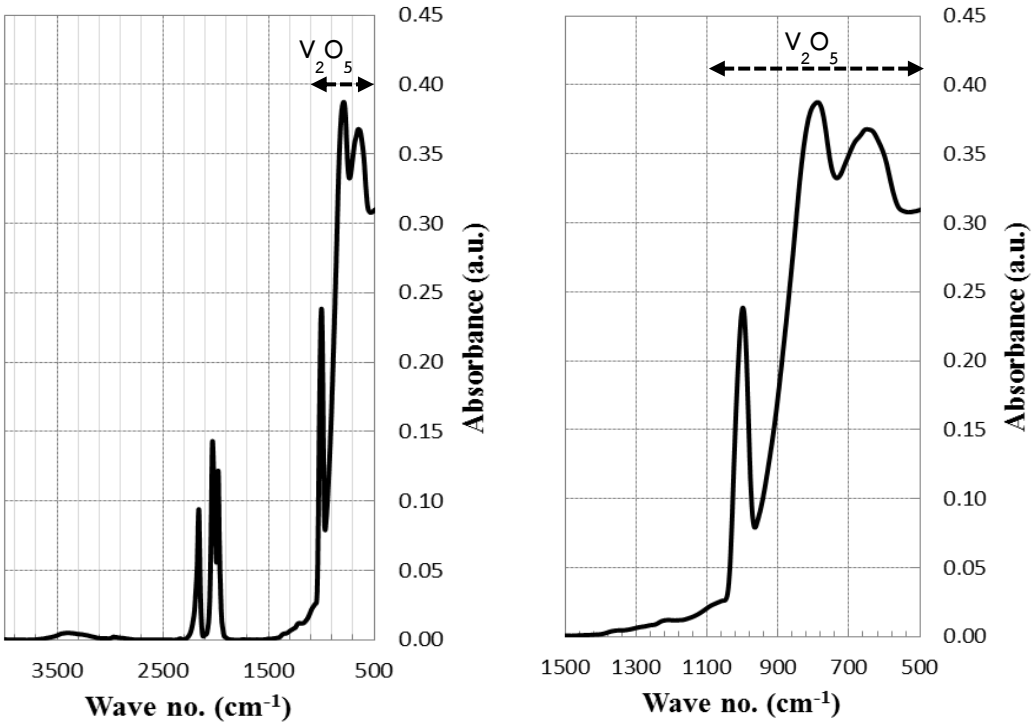

Figure 3.10 FT-IR spectrum of V_2O_5. (Piyanantarak, 2011)

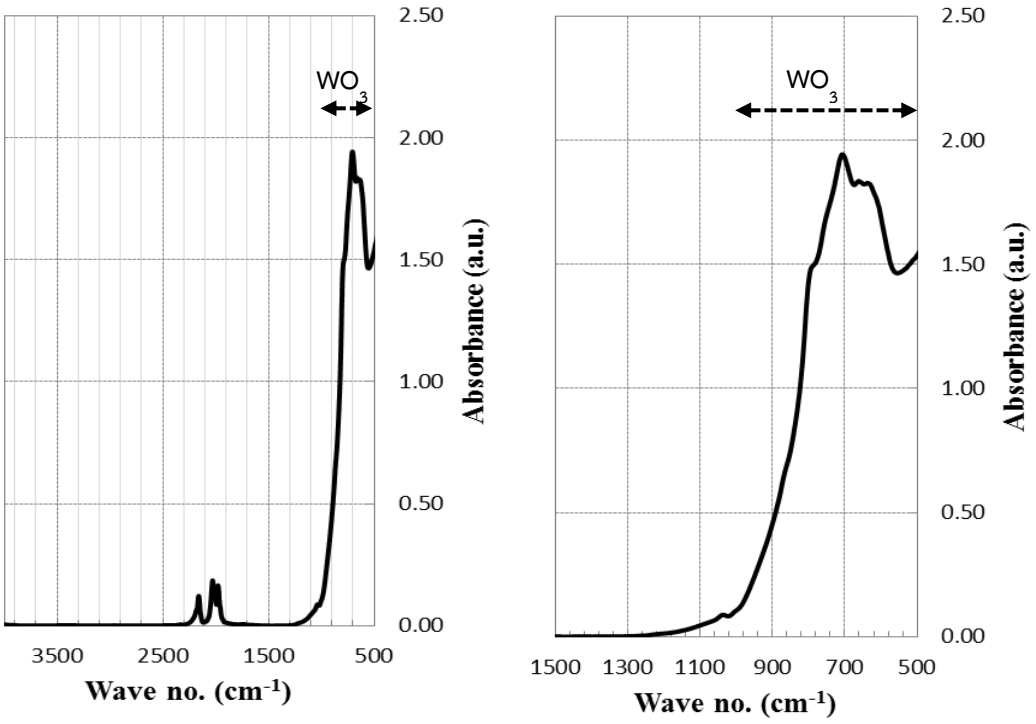

Figure 3.11 FT-IR spectrum of WO_3. (Piyanantarak, 2011)

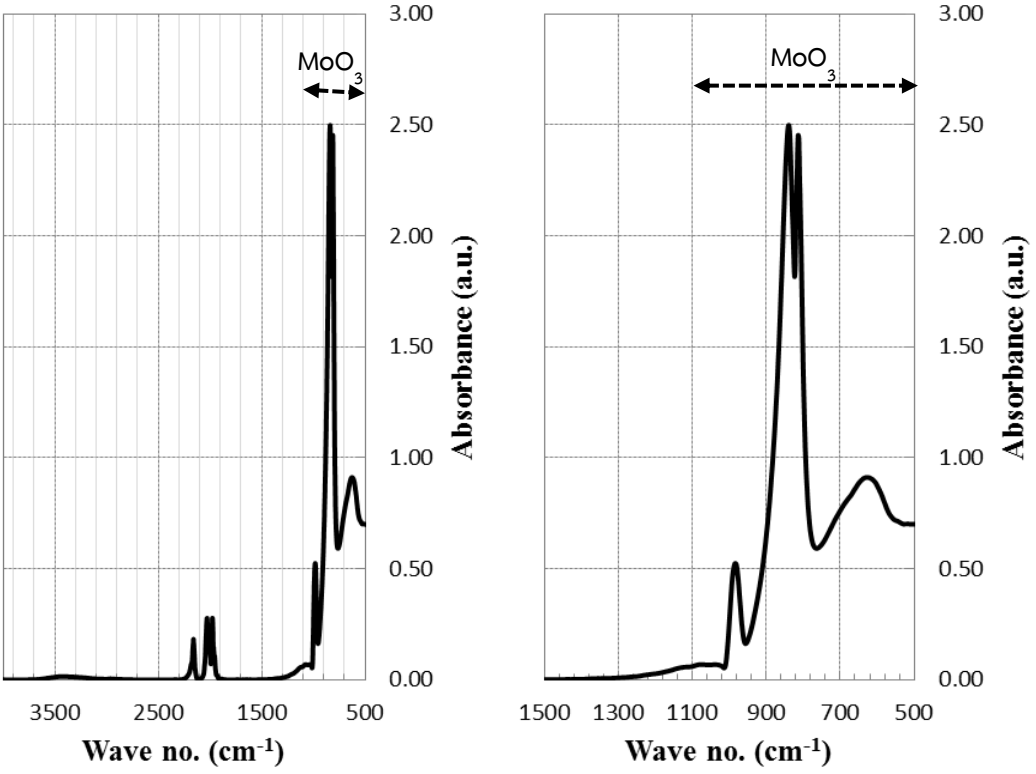

Figure 3.12 FT-IR spectrum of MoO_3. (Piyanantarak, 2011)

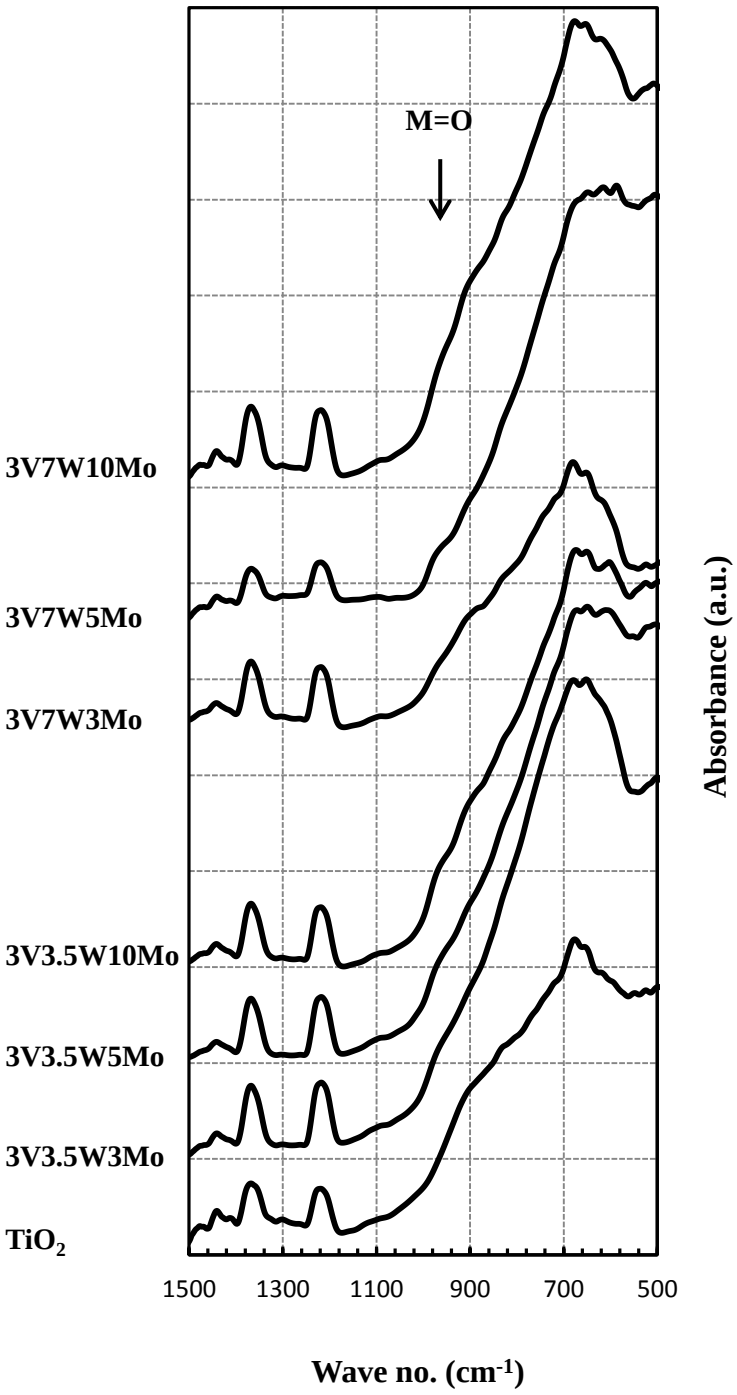

Figure 3.13 FT-IR spectra of the V_2O_5-WO_3-MoO_3/TiO_2 catalysts**.**

3.3 Catalytic activity testing

The previous work (Piyanantarak, 2011) shows that all catalyst used in this study can be reused several times without any deactivation or changing the properties. In this study the catalytic activity is measured from the formation of N_2O, oxidation of SO_2, oxidation of NH_3 and NO reduction using the catalysts prepared from the previous work (Piyanantarak, 2011).

Catalytic measurements have been carried out in a fixed bed stainless steel tubular reactor (I.D = 7 mm) with containing 0.1 g catalyst. Operate at atmospheric pressure and inserted into an electric furnace driven by a proportional-integral. Temperature of the furnace is controlled by a digital temperature controller. The diagram of the system is exhibited schematically in Figure 3.14. A feed consisting of 120 ppm NO, 120 ppm NH_3, 30 ppm SO_2, 15vol.% O_2,15vol.%H_2O with a nitrogen balance to make the total flow rate through the reactor was about 200 ml/min for NO removal and N_2O formation tests. In NH_3 oxidation reaction test was absent NO in feed stream and without NH_3 and H_2O in SO_2 oxidation test. Flow rate of each feed gas stream is controlled by using a set of mass flow controllers. In each run about 0.1 g of the prepared catalyst is tested by passing the feed gas stream through the catalyst bed packed on quartz wool. Activity data have been collected at different temperature in the range 120-450°C, each temperature was maintained for 1 hour, after steady-state condition were reached. For the analysis of NO and N_2O concentrations, the reactor outlet were connected in a gas chromatograph Shimadzu GC-2014 equipped with an electron capture detector (ECD). To analyze the SO_2 concentration in SO_2 oxidation reaction, the reactor outlet was connected in a gas chromatograph Shimadzu GC-2014 equipped with flame photometric detector (FPD).

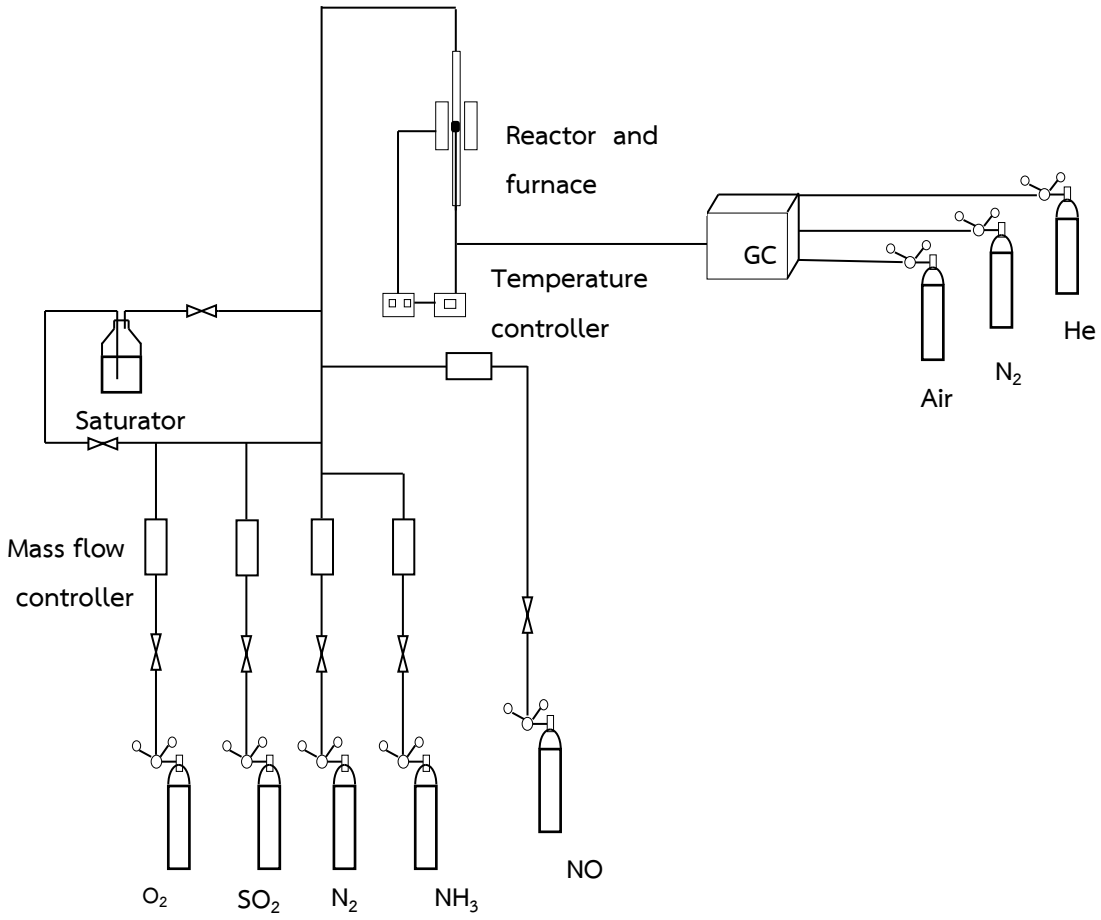

Figure 3.14 Flow diagram of the reactor system for SCR of NO by NH_3.

Table 3.5 The condition of gas chromatography.

Gas	Condition						
	Detector	**T_{column} (°C)**	**$T_{injector}$ (°C)**	**$T_{detector}$ (°C)**	**$P_{nitrogen}$** (kPa)	**P_{air}** (kPa)	**$P_{hydrogen}$** (kPa)
NO	ECD	40	200	200	240	-	-
N_2O	ECD	150	200	200	240	-	-
SO_2	FPD	180	100	185	-	35	105

ECD

Column max temperature:	190°C
Length:	2 m
Inner diameter:	0.10 mm ID
Film thickness:	1.00 µm
Sampling rate:	80 msec

FPD

Rt – XL Sulfur	
Column max temperature:	240°C
Length:	2 m
Inner diameter:	1 mm ID
Out diameter:	1/16 inch OD
Film thickness:	0.00 µm
Sampling rate:	40 msec

CHAPTER IV

RESULTS AND DISSCUSSION

4.1 Formation of SO_3 over V_2O_5-WO_3-MoO_3/TiO_2 catalysts

In the experiments of SO_2 oxidation, water was removed from the feed stream in order to avoid dissolution of SO_3 (if occurs) in condensed water vapor which may present in some part of tubing system where heating is not sufficient.

Figures 4.2 - 4.8 and table 4.1 show the concentration of SO_2 at the outlet of reactor of all V_2O_5-WO_3-MoO_3/TiO_2 catalysts and TiO_2 support. The results show that the concentration of SO_2 begins to decrease when the reaction temperature around 250°C. Even though TiO_2 is carried out in experimental the result also observed the concentration of SO_2 at the outlet of reactor decreased. Moreover, the SO_3 peak disappears on any chromatograms. These two phenomena (decrease of SO_2 when TiO_2 is used and disappearance of SO_3 peak) suggest that the reaction of SO_2 concentration at high temperature is not the result of the oxidation of SO_2 to SO_3. The real cause is the effect of the back pressure at the outlet of the SO_2 mass flow controller to increase with increasing the reactor temperature.

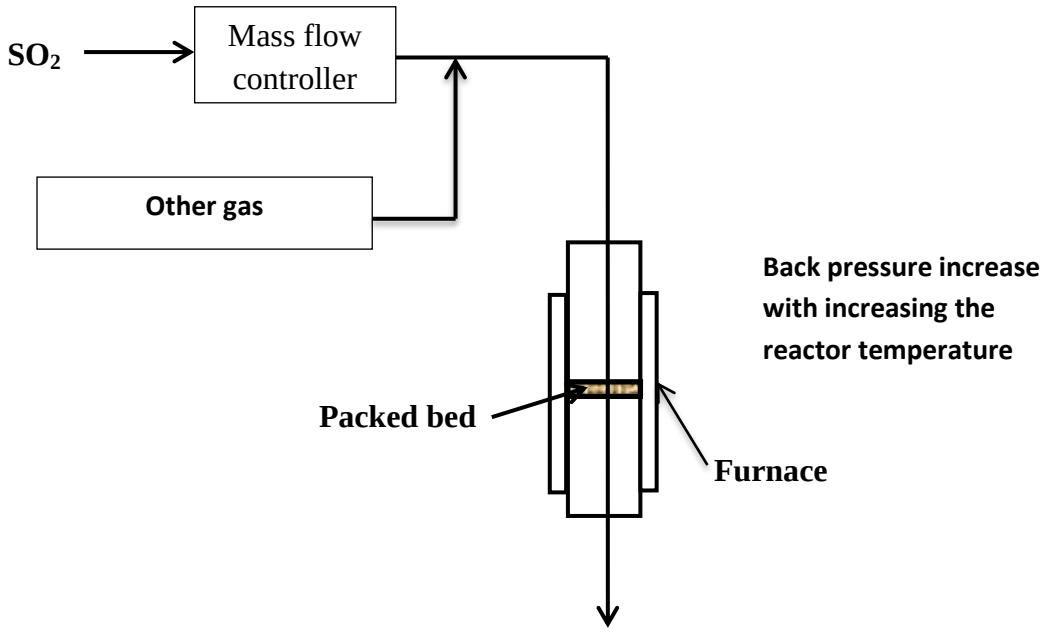

Figure 4.1 A simplified diagram of the reactor system.

The concentration of SO_2 used in our experiments is very low which leads to the valve opening of the SO_2 mass flow controller is therefore very low (0.45 from 10 full scale or equivalent to 0.6 ml/min at the supply pressure 2 barg). When the back pressure increases, the differential pressure across the valve decreases which results in the reduction of the actual flow rate of SO_2. This explanation is investigates by performing experiment by packing TiO_2 support having different pack density into the reactor. The higher pack density results in the higher back pressure. It is observed that the SO_2 mass flow controller will lose the capability to control the flow rate of SO_2 gas if the packed density is too high.

Therefore we can conclude that all the catalysts used in this research under the operating condition studies have insignificant SO_2 oxidation to SO_3 capability.

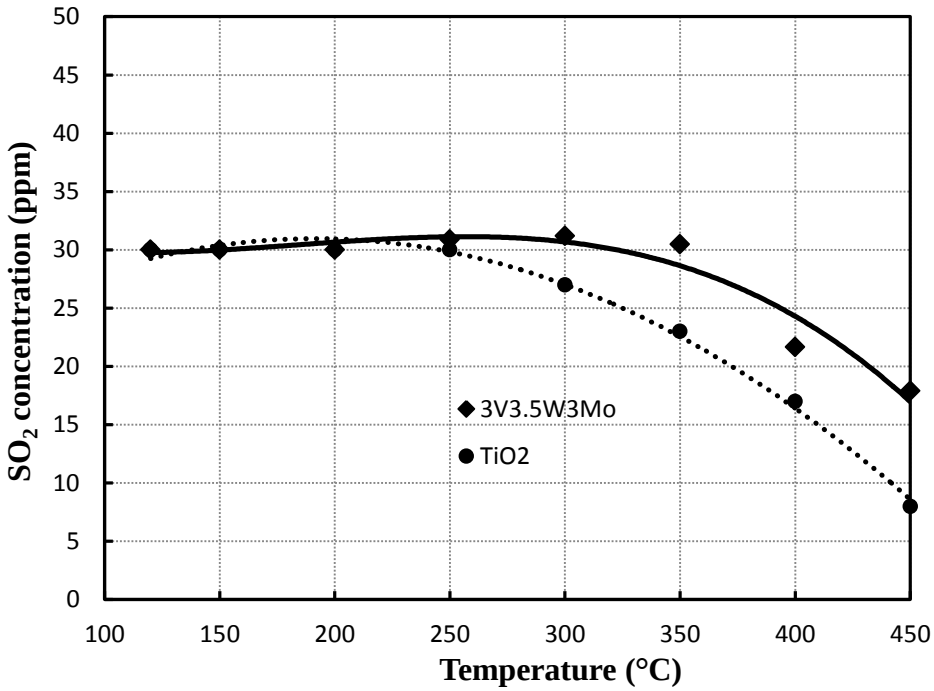

Figure 4.2 SO_2 oxidation over 3V3.5W3Mo/TiO_2 catalyst.

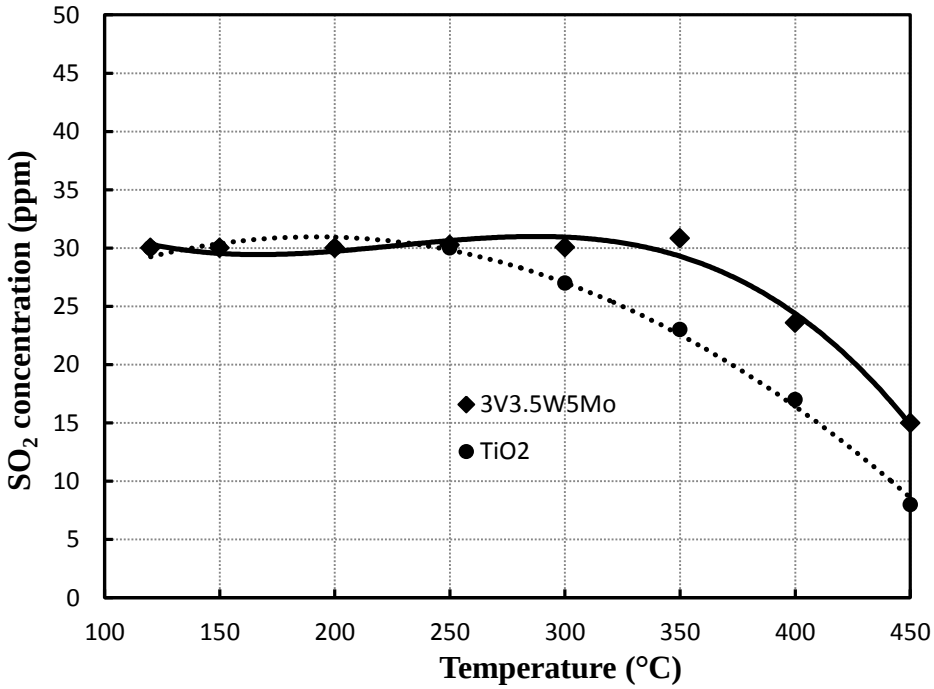

Figure 4.3 SO_2 oxidation over 3V3.5W5Mo/TiO_2 catalyst.

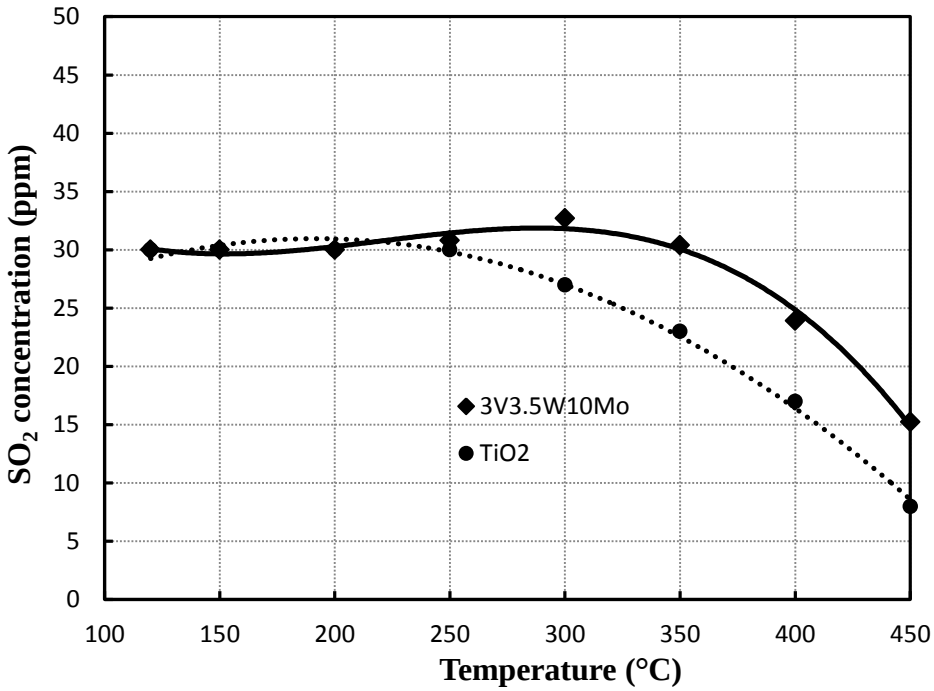

Figure 4.4 SO_2 oxidation over 3V3.5W10Mo/TiO_2 catalyst.

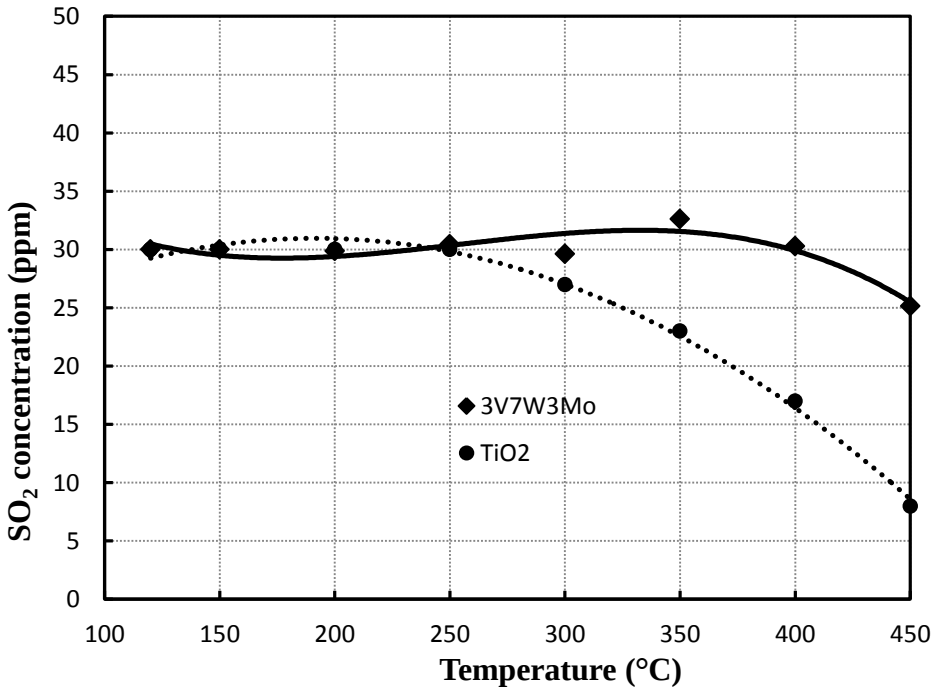

Figure 4.5 SO_2 oxidation over 3V7W3Mo/TiO_2 catalyst.

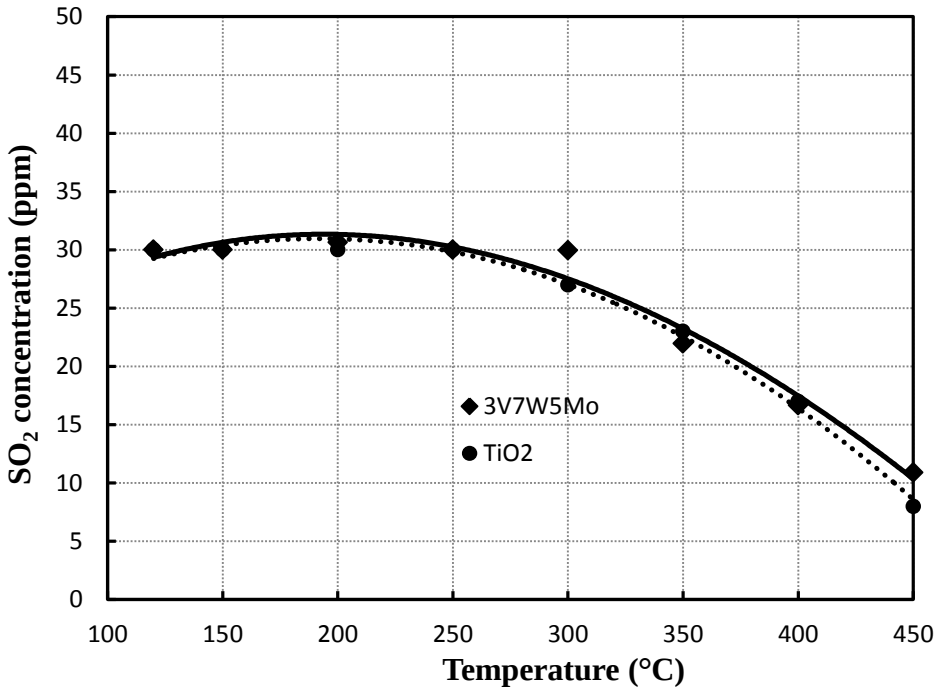

Figure 4.6 SO_2 oxidation over 3V7W5Mo/TiO_2 catalyst.

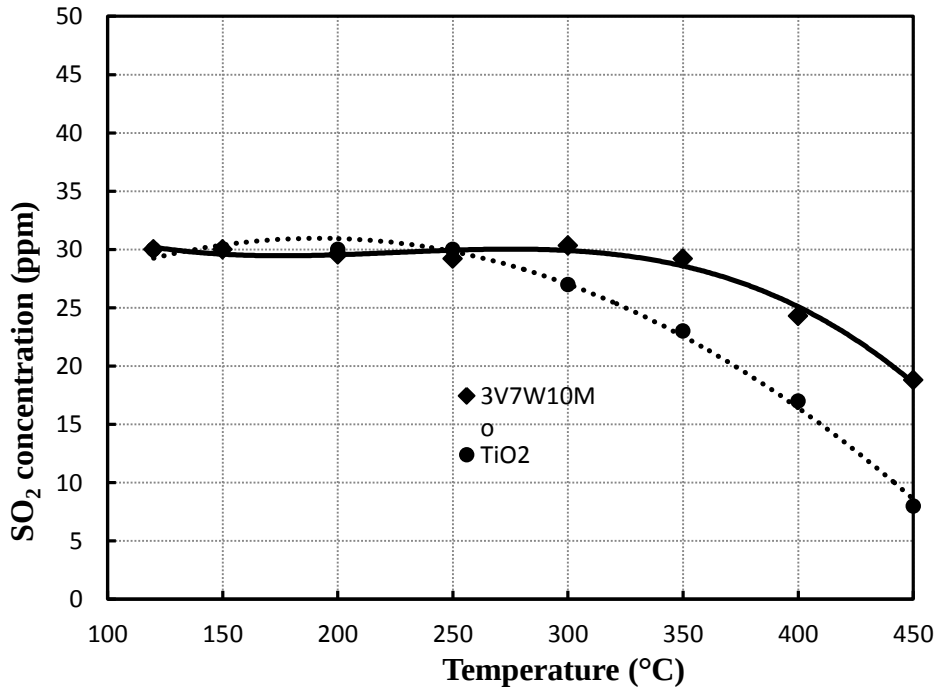

Figure 4.7 SO_2 oxidation over 3V7W10Mo/TiO_2 catalyst.

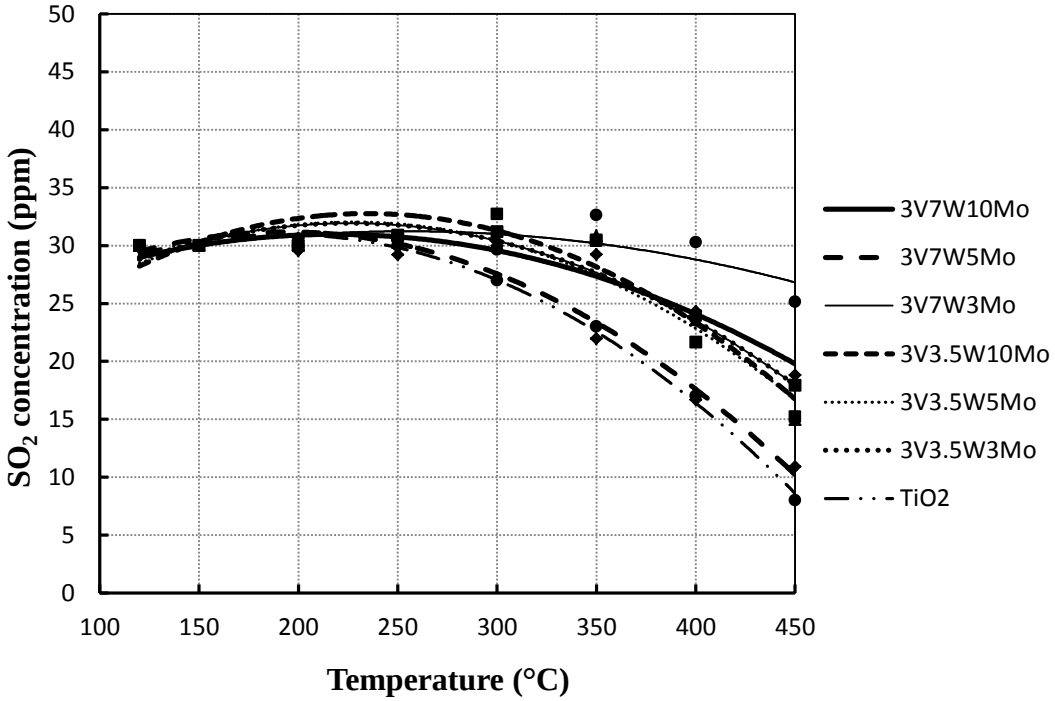

Figure 4.8 SO_2 oxidation over V_2O_5-WO_3-MoO_3/TiO_2 catalysts.

Table 4.1 SO_2 oxidation of V_2O_5-WO_3-MoO_3/TiO_2 catalysts.

Temperature	SO_2 concentration (ppm)						
(°C)	TiO_2	3V3.5W3Mo	3V3.5W5Mo	3V3.5W10Mo	3V7W3Mo	3V7W5Mo	3V7W10Mo
120	30.00	30.00	30.00	30.00	30.00	30.00	30.00
150	30.00	30.00	30.00	30.00	30.00	30.00	30.00
200	30.00	30.00	30.00	30.00	29.88	30.64	29.57
250	29.00	30.90	30.25	30.81	30.45	30.00	29.20
300	27.00	31.19	30.06	32.71	29.64	29.97	30.34
350	23.00	30.48	30.84	30.40	32.63	21.97	29.22
400	17.00	21.66	23.58	23.92	30.28	16.67	24.31
450	8.00	17.91	14.98	15.23	25.15	10.90	18.80

4.2 The behavior of V_2O_5-WO_3-MoO_3/TiO_2 catalysts

This section reports the catalytic behavior of all catalysts used in this study. The discussion on the reaction pathway is gathered in section 4.3. The results of NO conversion, NO from NH_3 oxidation and N_2O formation over V_2O_5-WO_3-MoO_3/TiO_2 catalysts show in figures 4.2-4.8.

4.2.1 The 3V3.5W3Mo/TiO_2 catalyst

NO conversion increase from 12.59% at 120°C to 100% at 200°C and remains at this level up to 300°C. Beyond 300°C, the NO conversion decreased continuously. The formation of N_2O appears between 300 - 400°C. The oxidation of NH_3 by O_2 begins when the reaction temperature is higher than 400°C.

Table 4.2 NO conversion, NO from NH_3 oxidation and N_2O formation over 3V3.5W3Mo/TiO_2 catalyst.

Temperature (°C)	NO conversion (%)	NO from NH_3 oxidation (ppm)	N_2O formation (ppm)
120	12.59	0.00	0.00
150	56.11	0.00	0.00
200	100.00	0.00	0.00
250	100.00	0.00	0.00
300	100.00	0.00	0.00
350	37.08	0.00	28.45
400	30.95	0.00	0.00
450	14.44	113.60	0.00

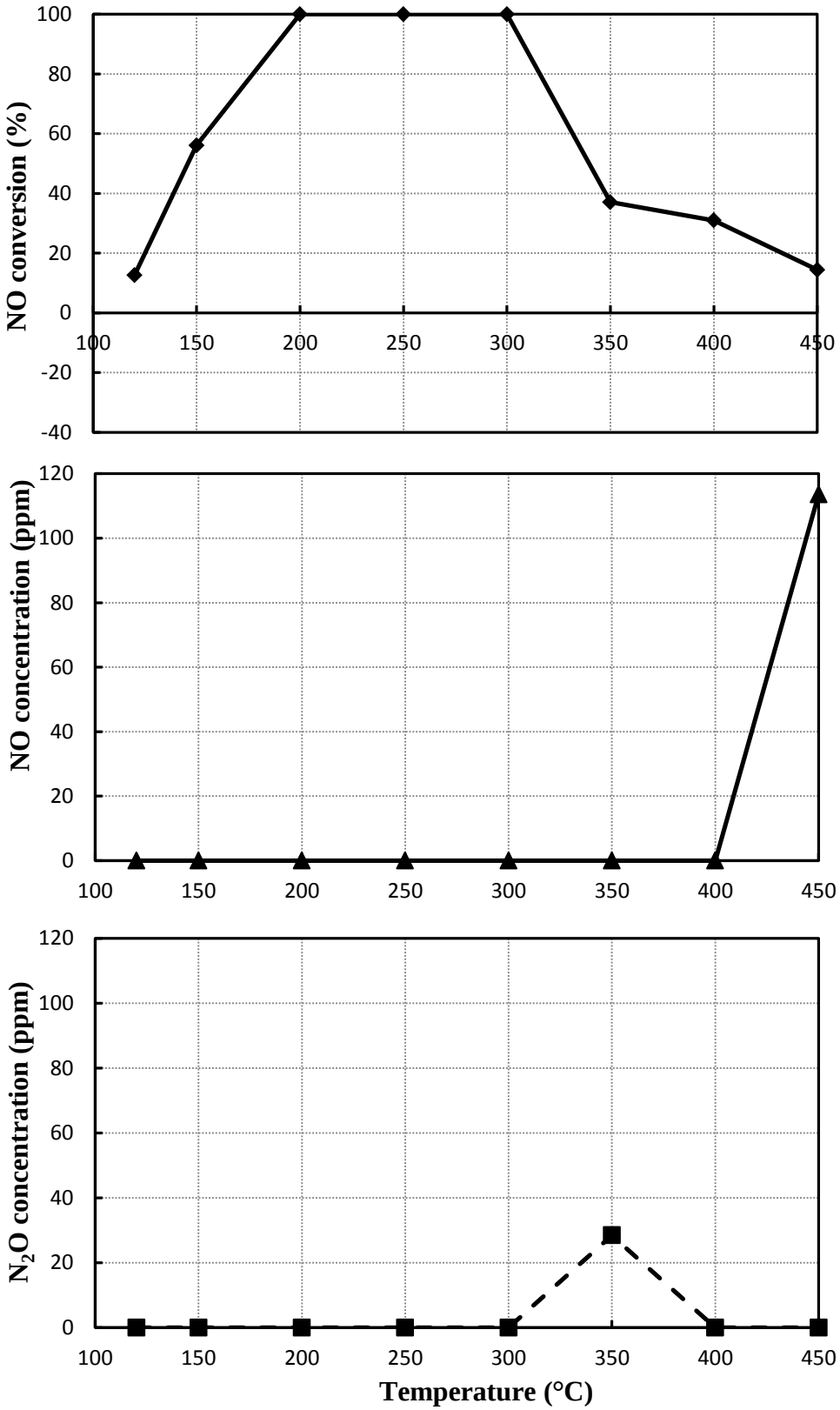

Figure 4.9 NO conversion, NO from NH_3 oxidation and N_2O formation over 3V3.5W3Mo/TiO_2 catalyst.

4.2.2 The 3V3.5W5Mo/TiO_2 catalyst

NO conversion increase from 38.80% at 120°C to 100% at 250°C and remains at this level up to 300°C. Beyond 300°C, the NO conversion decreased continuously to minus. The formation of N_2O disappears. The oxidation of NH_3 by O_2 begins when the reaction temperature is higher than 350°C.

Table 4.3 NO conversion, NO from NH_3 oxidation and N_2O formation over 3V3.5W5Mo/TiO_2 catalyst.

Temperature (°C)	**NO conversion (%)**	**NO from NH_3 oxidation (ppm)**	**N_2O formation (ppm)**
120	38.80	0.00	0.00
150	50.64	0.00	0.00
200	58.52	0.00	0.00
250	100.00	0.00	0.00
300	100.00	0.00	0.00
350	44.62	0.00	0.00
400	17.65	73.53	0.00
450	-21.31	88.24	0.00

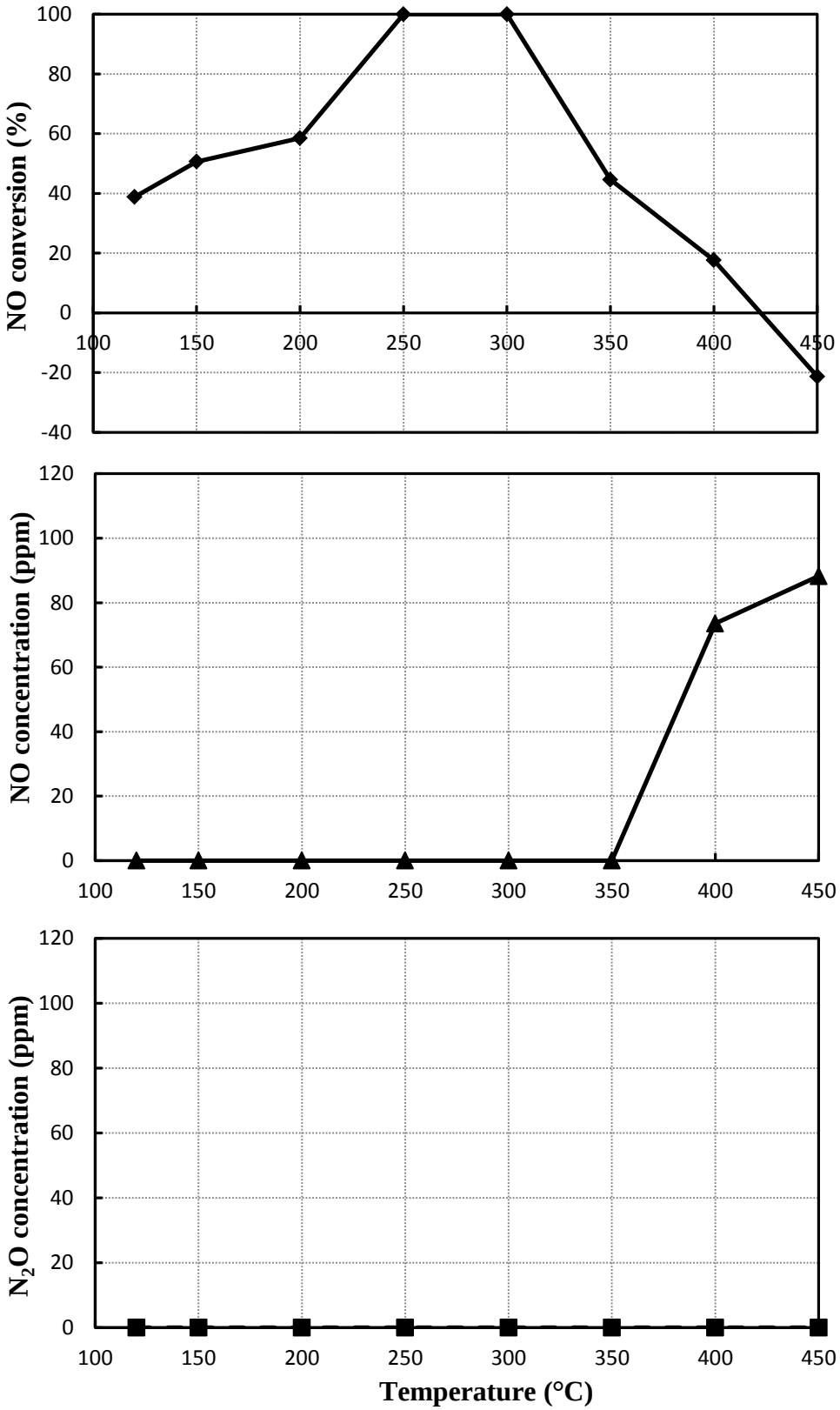

Figure 4.10 NO conversion, NO from NH_3 oxidation and N_2O formation over 3V3.5W5Mo/TiO_2 catalyst.

4.2.3 The 3V3.5W10Mo/TiO_2 catalyst

NO conversion increase from 2.04% at 120°C to 100% at 200°C and remains at this level up to 300°C. Beyond 300°C, the NO conversion decreased steadily to severely minus. The formation of N_2O appears between 200 - 400°C. The oxidation of NH_3 by O_2 begins when the reaction temperature is higher than 300°C.

Table 4.4 NO conversion, NO from NH_3 oxidation and N_2O formation over 3V3.5W10Mo/TiO_2 catalyst.

Temperature (°C)	**NO conversion (%)**	**NO from NH_3 oxidation (ppm)**	**N_2O formation (ppm)**
120	2.04	0.00	0.00
150	54.67	0.00	0.00
200	100.00	0.00	0.00
250	100.00	0.00	28.38
300	100.00	0.00	0.00
350	9.57	43.27	27.78
400	-43.62	96.60	0.00
450	-76.29	120.00	0.00

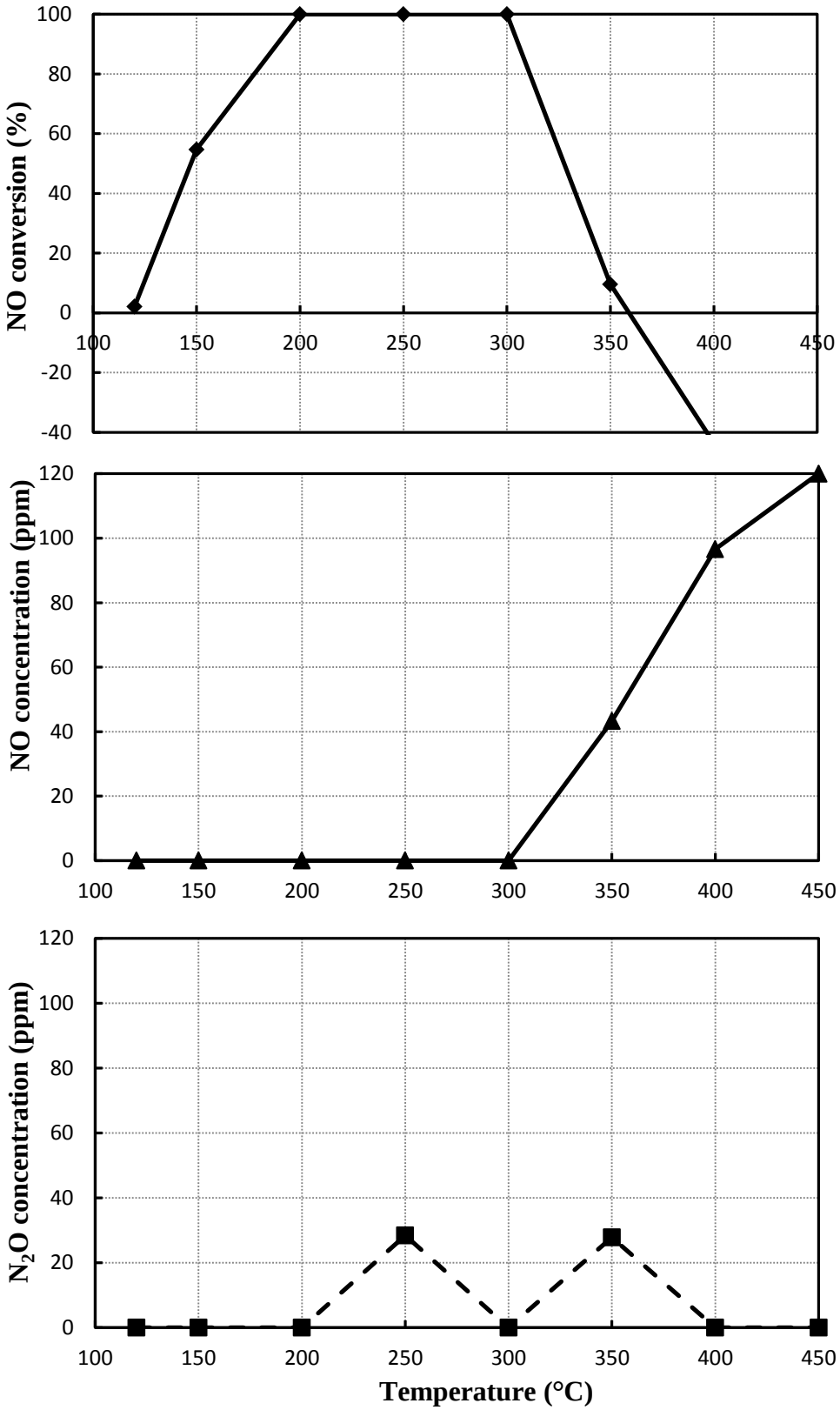

Figure 4.11 NO conversion, NO from NH_3 oxidation and N_2O formation over 3V3.5W10Mo/TiO_2 catalyst.

4.2.4 The 3V7W3Mo/TiO_2 catalyst

NO conversion increase from 43.09% at 120°C to 100% at 250°C and remains at this level up to 350°C. Beyond 350°C, the NO conversion decreased continuously. The formation of N_2O appears between 200 - 350°C. The oxidation of NH_3 by O_2 begins when the reaction temperature is higher than 300°C.

Table 4.5 NO conversion, NO from NH_3 oxidation and N_2O formation over 3V7W3Mo/TiO_2 catalyst.

Temperature (°C)	**NO conversion (%)**	**NO from NH_3 oxidation (ppm)**	**N_2O formation (ppm)**
120	43.09	0.00	0.00
150	46.40	0.00	0.00
200	78.55	0.00	0.00
250	100.00	0.00	8.15
300	100.00	0.00	21.45
350	100.00	62.14	0.00
400	79.71	83.22	0.00
450	28.30	103.81	0.00

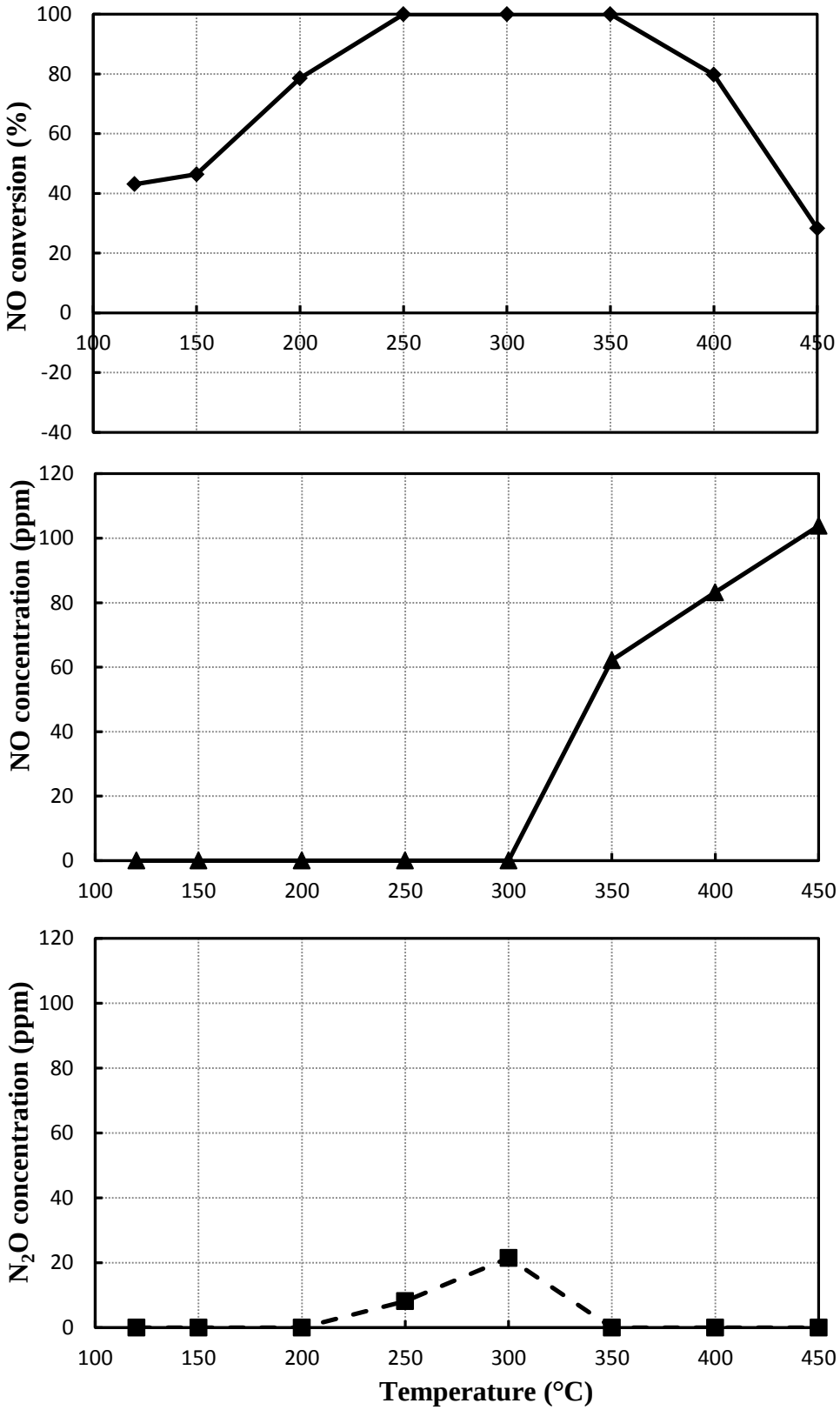

Figure 4.12 NO conversion, NO from NH_3 oxidation and N_2O formation over 3V7W3Mo/TiO_2 catalyst.

4.2.5 The 3V7W6Mo/TiO_2 catalyst

NO conversion increase from 14.62% at 120°C to 100% at 300°C and remains at this level up to 350°C. Beyond 350°C, the NO conversion decreased continuously. The formation of N_2O appears between 250 - 400°C. The oxidation of NH_3 by O_2 begins when the reaction temperature is higher than 350°C.

Table 4.6 NO conversion, NO from NH_3 oxidation and N_2O formation over 3V7W5Mo/TiO_2 catalyst.

Temperature (°C)	**NO conversion (%)**	**NO from NH_3 oxidation (ppm)**	**N_2O formation (ppm)**
120	14.62	0.00	0.00
150	26.78	0.00	0.00
200	60.24	0.00	0.00
250	86.70	0.00	0.00
300	100.00	0.00	39.76
350	100.00	0.00	26.36
400	80.32	95.96	0.00
450	2.18	105.99	0.00

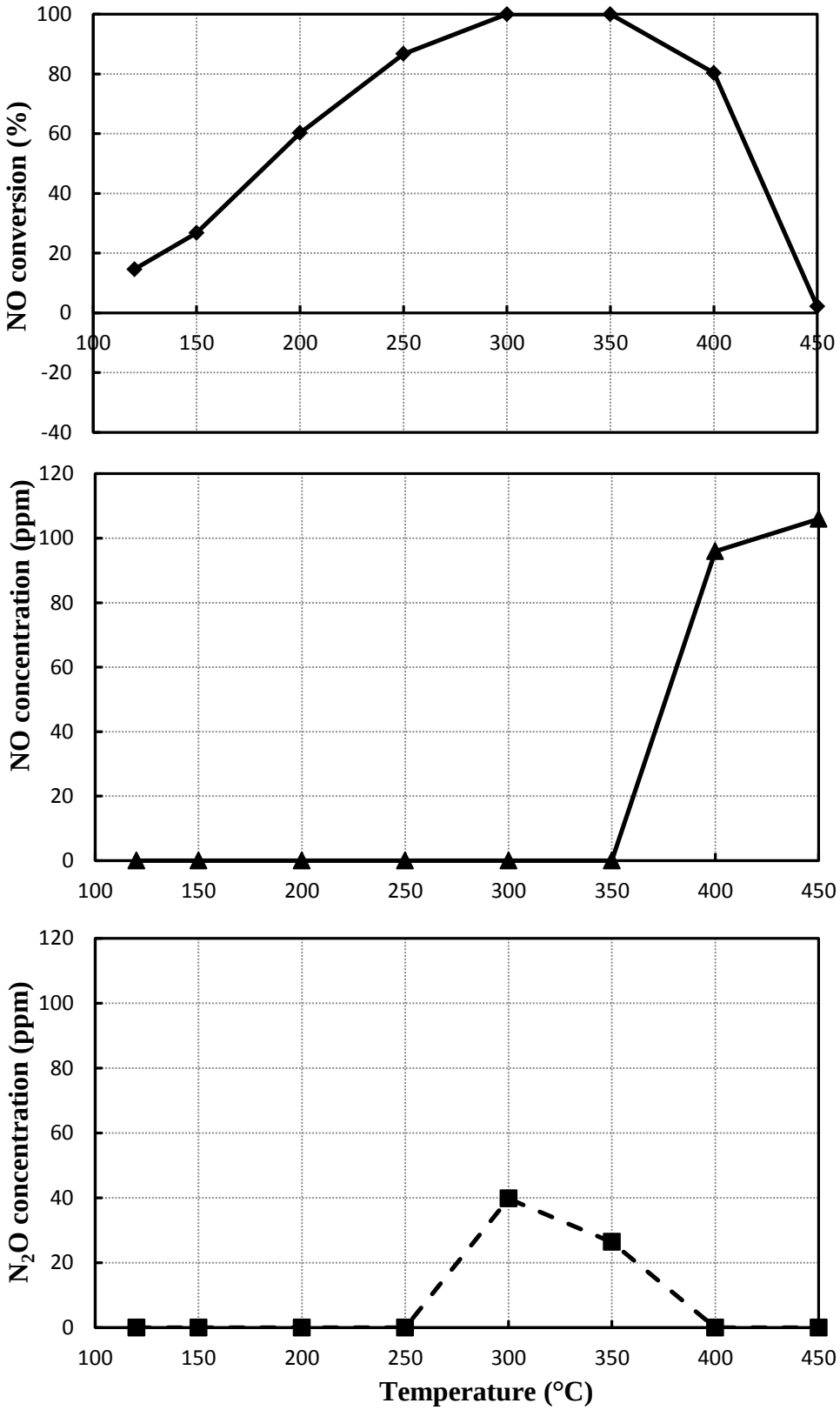

Figure 4.13 NO conversion, NO from NH_3 oxidation and N_2O formation over 3V7W5Mo/TiO_2 catalyst.

4.2.6 The 3V7W10Mo/TiO_2 catalyst

NO conversion increase from 40.99% at 120°C to 100% at 200°C and remains at this level up to 300°C. Beyond 300°C, the NO conversion decreased continuously. The formation of N_2O appears between 300 - 450°C. The oxidation of NH_3 by O_2 begins when the reaction temperature is higher than 350°C.

Table 4.7 NO conversion, NO from NH_3 oxidation and N_2O formation over 3V7W10Mo/TiO_2 catalyst.

Temperature (°C)	**NO conversion (%)**	**NO from NH_3 oxidation (ppm)**	**N_2O formation (ppm)**
120	40.99	0.00	0.00
150	61.23	0.00	0.00
200	100.00	0.00	0.00
250	100.00	0.00	0.00
300	100.00	0.00	0.00
350	79.25	0.00	17.05
400	35.15	89.18	13.68
450	28.56	98.97	0.00

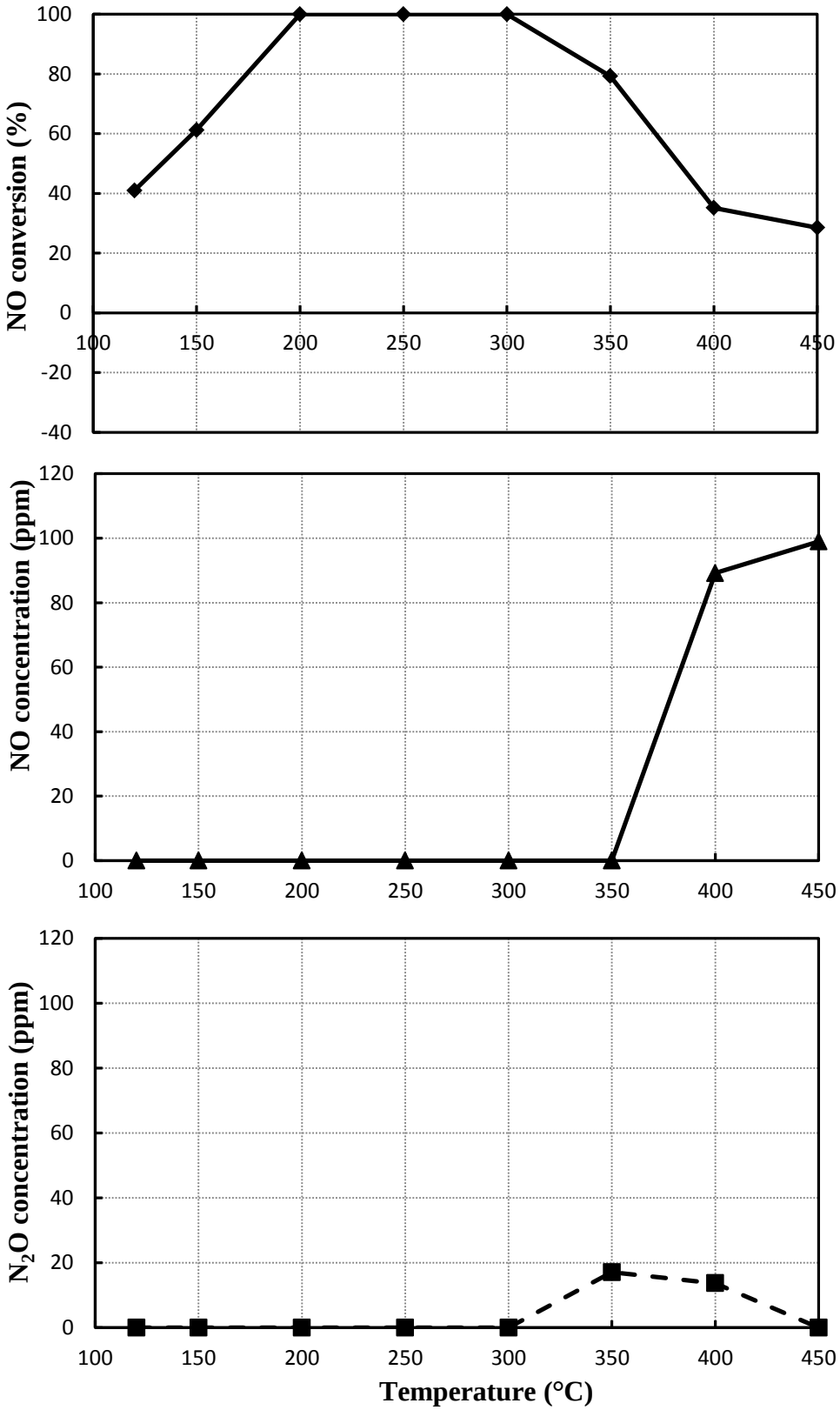

Figure 4.14 NO conversion, NO from NH_3 oxidation and N_2O formation over 3V7W10Mo/TiO_2 catalyst.

4.3 The SCR reaction pathway of V_2O_5-WO_3-MoO_3/TiO_2 catalysts

During the SCR process we hypothesize the reactions can occur that

1. Adsorption of NH_3 on catalysts surface. NO from gas phase reacts with NH_3.

2. Adsorption of NH_3 on catalysts surface. O_2 from gas phase react with NH_3.

The reactions 1 and 2 follow the Eley–Rideal mechanism. But this mechanism is limited by the ability of catalyst surface to maintain NH_3 molecule which illustrated in NH_3 –TPD. The ability of catalyst surface to adsorb NH_3 can be quantified from NH_3–TPD results. This mechanism is not likely at high temperature.

3. NH_3 molecules react with lattice oxygen on catalyst surface result in the reduction of the catalyst surface. Then NO molecule oxidized the catalyst surface back to the normal state.

4. NH_3 molecule reacts with lattice oxygen on catalyst surface result in the reduction of the catalyst surface. Then O_2 molecule oxidized the catalyst surface back to the normal state.

Reactions 3 and 4 follow the redox mechanism this mechanism not likely occurred at low temperature.

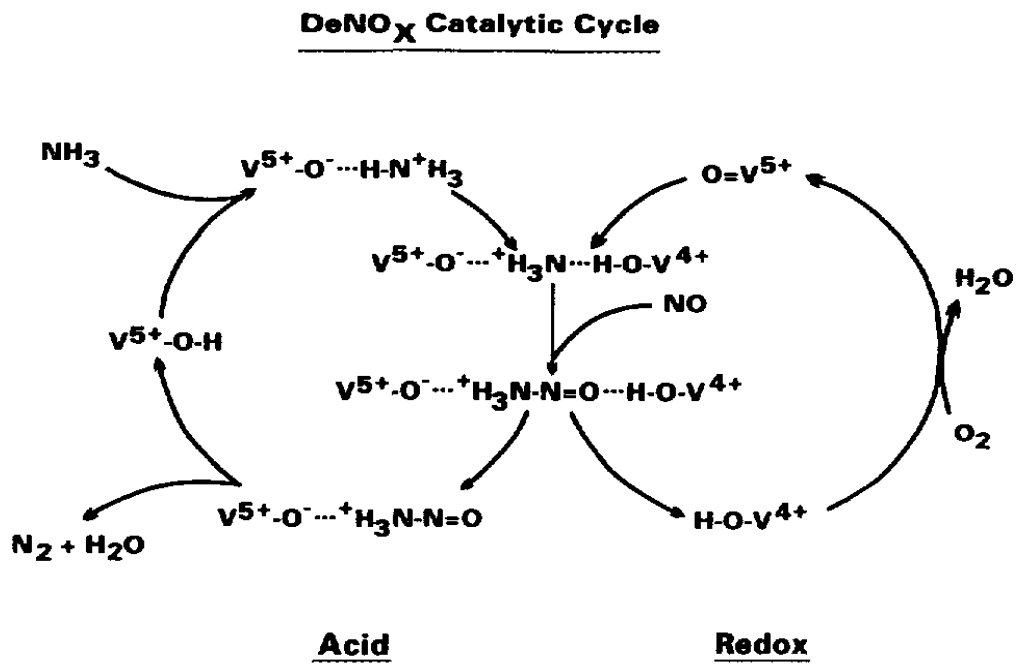

Figure 4.15 Catalytic cycle of the SCR reaction over V_2O_5/TiO_2 catalyst. (Topsϕe et al., 1995)

Topsϕe et al. (1995) suggested the mechanism in SCR process. The $DeNO_x$ catalytic cycle is consists of significantly two reaction cycle. There are acid and redox cycle. The $DeNO_x$ cycle is proposed by NH_3 adsorption on bronsted acid sites or V^{5+} - OH. Adsorbed NH_3 is then activated by the transfer of H atom to the V^{5+}= O and is reduced to V^{4+}- OH at the same time. NO from the gas phase reacts with the activated NH_3 molecule or weakly adsorbed species. The reaction product released from the surface are N_2 and H_2O. The V^{5+}- OH was directly back into the $DeNO_x$ cycle and the V^{4+}- OH was reoxidized to the V^{5+}= O site by O_2.

5. Homogeneous reaction. NH_3 react with NO in gas phase.

6. Homogeneous reaction. NH_3 react with O_2 in gas phase.

The homogeneous is not depending on the catalyst but depending on the temperature. Then this mechanism occurred at high temperature.

Since the presence of NH_3 is necessary to the reduce NO then if the high NO conversion observed for example achieved 100% therefore another reaction have the NH_3 involving not occurred.

4.3.1 The SCR reaction in a low temperature region

The definition of low reaction temperature in the present work is from 120°C to the temperature that is NO conversion has the highest. The mechanism in the low reaction temperature region in our opinion is the Eley–Rideal mechanism which seems to be more reasonably. Because the surface of metal oxide consists of cation and anion species, these species prefer to adsorb polar molecule such as NH_3 and H_2O. The adsorption of nonpolar molecules such as O_2, NO on metal oxide surface can occur if the oxide surface is oxidized or reduced. (Bond, 1987)

In our case, the metal oxide (V_2O_5, WO_3 and MoO_3) are in their highest oxidation state. The adsorption of the nonpolar molecule (O_2, NO) can occurred where this reduce to lower oxide state. They meaning of reduction here is a loss of O^{2-} anion to O_2 without the involvement of any reducing agent (NH_3). This reduction process normally requires high temperature in the order of several hundred degree celcius. Figure 4.16 illustrate the decomposition of MgO at high temperature.

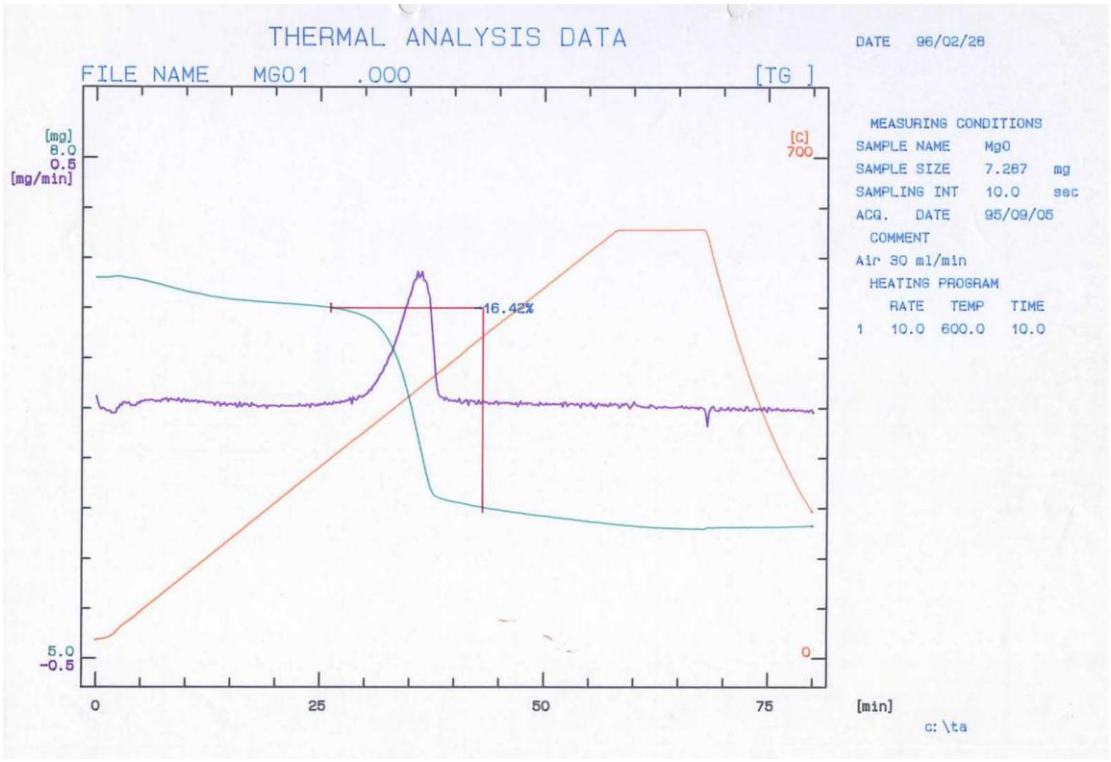

Figure 4.16 The decomposition of MgO. (Thammanonkul, 1996)

Therefore, the reactions in low temperature range are 1 and 2 that are the Eley–Rideal mechanism. If we look at the NO conversion curve and NH_3 oxidation curve, it can see that the oxidation of NH_3 by O_2 (in absence NO) at reaction temperature higher than the reduction of NO.

4.3.2 The SCR reaction in a high temperature region

At high temperature the amount of adsorbed NH_3 remains on the catalyst surfaces decreased. This phenomenon leads to low reaction rates. On the contrary, the increase of rate constant leads to rate of reaction increases. Then the overall rate of reaction depends on with factor play the dominate reaction.

For the 3V3.5W5Mo catalyst, it can see the NO conversion significantly rapidly about 350°C while no observed the formation of N_2O and the NH_3 oxidation still not apparent. From this example, it indicate that the amount of adsorb NH_3 on catalyst surface lead to decrease of NO conversion more increasing of rate constant of SCR process.

For other catalyst the decrease of NO conversion at high temperature is more complicated due to the formation of N_2O. In order to explain the behavior of catalysts (3V3.5W3Mo, 3V3.5W10Mo, 3V7W3Mo, 3V7W5Mo and 3V7W10Mo) in high temperature region then we should firstly consider the formation of N_2O.

4.3.3 N_2O formation in during SCR reaction

The possible reaction for the formation of N_2O can be the reaction between NH_3 and NO or the oxidation between NH_3 and O_2. If NH_3 react with O_2 we shall lost part of NH_3 then the reaction of NO by NH_3 cannot achieve 100% if N_2O forms from NH_3 react with O_2. Oxidation of NH_3 to NO occurred after N_2O formation.

The temperature of N_2O formation and the temperature of NO conversion in SCR process achieve 100% are overlap. But the result of the behaviors of the catalyst (3V3.5W10Mo, 3V7W3Mo and 3V7W5Mo) show that the formation of N_2O occurred in the temperature range of NO conversion achieved 100%. Therefore, the result of these catalysts indicated that the formation of N_2O occurred from NO reacts with NH_3 to produce N_2O.

For 3V3.5W3Mo and 3V7W11Mo catalysts, the formations of N_2O appear in during the NO conversion drop because of two dominant factors that are:

1) The amount of adsorbed NH_3 over catalyst surface decrease.

2) Formation of N_2O from NO reacts with NH_3 more from oxidation of NH_3.

4.3.4 Oxidation of NH_3 by O_2

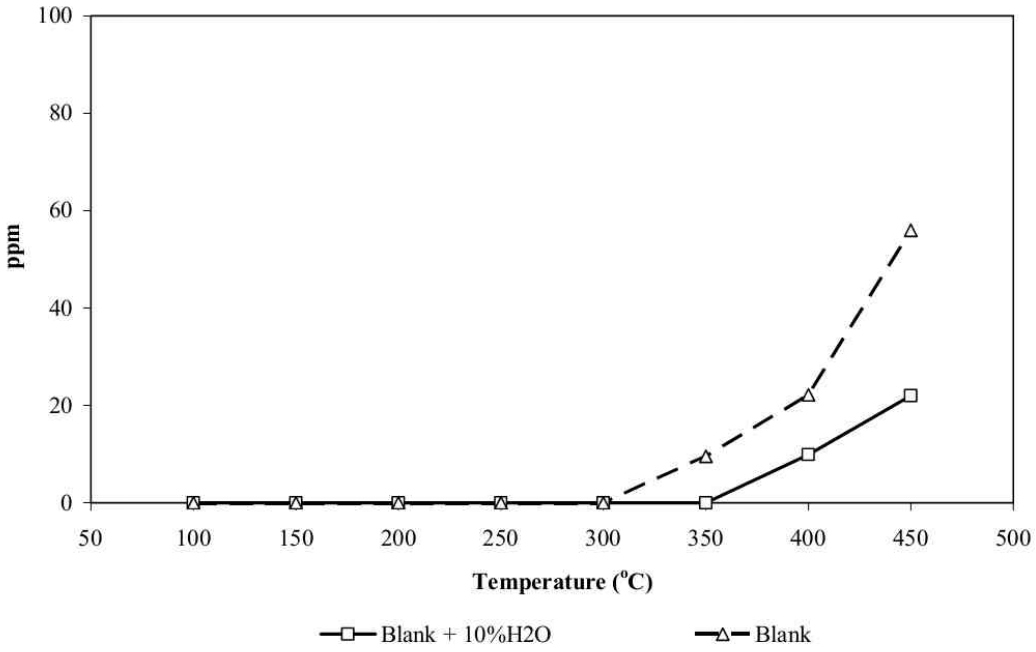

Figure 4.17 Ammonia oxidation in blank reactor for SCR of NO by NH_3. (Kaewbuddee, 2009)

The homogeneous reaction between NH_3 and O_2 to NO is an avoidable at high temperature. The experimental carried out using the same equipment under the same operating condition, However figure 4.17 shows that the formation of NO from the homogeneous reaction is lower than was observed during catalytic reaction. Therefor there must be at least one catalytic partway that contribute to the formation of NO from NH_3.

The NH_3 –TPD results reported previous in chapter IIV review that at 450°C the no adsorbed NH_3 species on catalysts surface (3V3.5W10Mo, 3V7W5Mo and 3V7W10Mo) or the amount of adsorbed NH_3 species on catalysts surface (3V3.5W3Mo, 3V3.5W5Mo and 3V7W3Mo) are low but the oxidation of NH_3 to NO of all catalysts is not different. The results of NH_3 oxidation is shown in figure 4.18.

Therefor the adsorption of NH_3 (Eley–Rideal mechanism) is not the route for the oxidation of NH_3 but it is probably the REDOX mechanism.

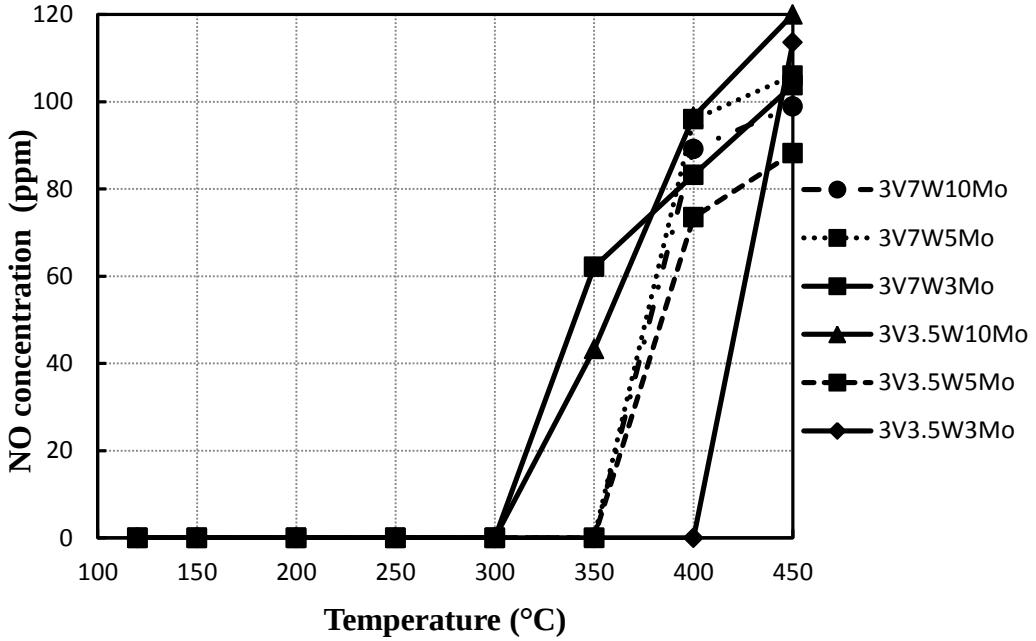

Figure 4.18 NO concentration from NH_3 oxidation as function of reaction temperature over V_2O_5-WO_3-MoO_3/TiO_2 catalysts.

Table 4.8 NO concentration from NH_3 oxidation of V_2O_5-WO_3-MoO_3/TiO_2 catalysts.

Temperature (°C)	**NO concentration (ppm)**					
	3V3.5W3Mo	**3V3.5W5Mo**	**3V3.5W01Mo**	**3V7W3Mo**	**3V7W5Mo**	**3V7W10Mo**
120	0.00	0.00	0.00	0.00	0.00	0.00
150	0.00	0.00	0.00	0.00	0.00	0.00
200	0.00	0.00	0.00	0.00	0.00	0.00
250	0.00	0.00	0.00	0.00	0.00	0.00
300	0.00	0.00	0.00	0.00	0.00	0.00
350	0.00	0.00	43.27	62.14	0.00	0.00
400	0.00	73.53	96.60	83.22	95.96	89.18
450	113.60	88.24	120.00	103.81	105.99	98.97

CHAPTER V

CONCLUSIONS AND RECOMMENDATIONS

In this chapter, section 5.1 provides the conclusions obtained from the experimental results. Furthermore, recommendations for further study are given in section 5.2.

5.1 Conclusions

From the experimental report and the discussions above the following conclusions can be drawn.

In the SCR process, the Eley–Rideal mechanism determined the activity of the SCR reaction in a low temperature region. On the other hand the amount of adsorbed NH_3 on surface catalysts determined the NO conversion in the high temperature region.

The formation of N_2O causes from NO reacts with adsorbed NH_3 following the Eley–Rideal mechanism.

The oxidation of NH_3 by O_2 appears via homogeneous and redox mechanism.

The oxidation of SO_2 to SO_3 does not occur but the SO_2 concentration in the outlet gas decrease with increasing the reaction temperature because of back pressure over packed bed.

5.2 Recommendation for future work

In the future we should study the formation of N_2O by V_2O_5-WO_3-MoO_3/TiO_2 catalysts. To find a catalyst which minimize the production of N_2O.

REFERENCES

Amiridis, M. D.,Wachs, I. E., Deo, G., Jehng, J.-M. and Kim, D.S. Reactivity of V_2O_5 catalysts for the selective catalytic reduction of NO by NH_3 : Influence of vanadia loading, H_2O and SO_2. Journal of catalysis 161(1996): 247-253.

Bond, G.C. Heterogeneous catalysis: principles and application 2nd ed., Oxford Universiyy Press (1987): 62-64.

Busca, G., Lietti, L., Ramis, G. and Berti, F. Chemical and mechanistic aspects of the selective catalytic reduction of NO_x by ammonia over oxide catalysts: A review. Applied Catalysis B: Environmental 18 (1998): 1-36.

Casagrande, L., Lietti, L., Nova, I., Forzatti, P. and Baiker, A. SCR of NO by NH_3 over TiO_2-supported V_2O_5-MoO_3 catalysts: reactivity and redox behavior. Applied Catalysis B: Environmental 22 (1999): 63-77.

Forzatti, P., Nova, I. and Beretta, A. Catalytic properties in deNO_x and SO_2 –SO_3 reactions. Catalytic Today 56 (2000): 431-441.

Forzatti, P., Nova, I., Tronconi, E., Kustov, A. and Thogersen, J.R. Effect of operating variables on the enhanced SCR reaction over a commercial V_2O_5–WO_3/TiO_2 catalyst for stationary applications. Catalysis Today 184 (2012): 153– 159.

Giakoumelou, I., Fountzoula, C., Kordulis, C. and Boghosian, S. Molecular structure and catalytic activity of V_2O_5/TiO_2 catalysts for the SCR of NO by NH_3: In situ Raman spectra in the presence of O_2, NH_3, NO, H_2, H_2O and SO_2. Journal of catalysis 239 (2006): 1-12.

Jehng, J.-M., Deo, G., Weckhuysen, B.M. and Wachs, I.E. Effect of water vapor on the molecular structures of supported vanadium oxide catalysts at elevated temperatures. Journal of Molecular Catalysis A: Chemical 10 (1996): 41-54.

Kaewbuddee, C. Selective catalytic reduction of nitrogen oxide by ammonia over V_2O_5-WO_3/TiO_2 catalysts. Master's Thesis, Department of Chemical Engineering, Faculty of Engineering, Chulalongkorn University. (2009)

Kamata, H., Ohara, H., Takahashi, K., Yukimura, A. and Seo, Y. SO_2 oxidation over the V_2O_5/TiO_2 SCR catalyst. Catalysis Letters 73 (2001)

Lietti, L., Alemany, J.L., Forzatti, P., Busca, G., Ramis, G., Giamello, E. and Bregani, F. Reactivity of V_2O_5-WO_3/TiO_2 catalysts in the selective catalytic reduction of nitric oxide by ammonia. Catalysis Today 29 (1996): 143-148.

Lee, S.M., Kim, S.S. and Hong, S.C. Systemmatic mechanism study of the high temperature SCR of NO_x by NH_3 over a W/TiO_2 catalyst. Chemical Engineering Science 79 (2012): 177-185.

Martin, J. A., Yates, M., Avila, P., Suarez, S., and Blanco, J. Nitrous oxide formation in low temperature selective catalytic reduction of nitrogen oxides with V_2O_5/TiO_2 catalysts. Applied Catalysis B: Environmental 70 (2007): 330-334.

Nova, I., Lietti, L., Casagrande, L., Dall'Acqua, L., Giamello, E. and Forzatti, P. Characterization and reactivity of TiO_2-supported MoO_3 de-NO_x SCR catalysts. Applied Catalysis B: Environmental 17 (1998): 245-258.

Nova, I., dall'Acqua, L., Lietti, L., Giamello, E. and Forzatti, P. Study of thermal deactivation of a de-NO_x commercial catalyst. Applied Catalysis B: Environmental 35 (2001): 31-42.

Orsenigo, C., Beretta, A., Forzatti, P., Svachula, J. Theoretical and experimental study of the interaction between NO_x reduction and SO_2 oxidation over DeNO_x-SCR catalysts. Catalysis Today 27 (1996): 15-21.

Pena, D. A., Uphade, B. S. and. Smirniotis, P. G. TiO_2-supported metal oxide catalysts for low-temperature selective catalytic reduction of NO with NH_3 I. Evaluation and characterization of first row transition metals. Journal of Catalysis, 221 (2004): 421–431.

Piyanantarak, B. Selective catalytic reduction of nitrogen oxide by ammonia over V_2O_5-WO_3-MoO_3/TiO_2 catalysts. Master's Thesis, Department of Chemical Engineering, Faculty of Engineering, Chulalongkorn University. (2011)

Svachula, J., Alemany, L.J., Ferlazzo, N., Forzatti, P. and Tronconi, E. Oxidation of SO_2 to SO_3 over honeycomb denoxing catalysts. Ind.Eng.Chem.Res 32 (1993): 826-834.

Thammanonkul H. Oxidative dehydrogenation of propane over V-Mg-O catalysts. Master's Thesis, Department of Chemical Engineering, Faculty of Engineering, Chulalongkorn University. (1996)

Topsoe, N.-Y. Dumesic, J.A. and Topsoe H. Vanadia/Titania catalysts for selective catalytic reduction of nitric oxide by ammonia. Journal of Catalysis 151 (1995): 241-252.

Wong, W.C. and Nobe, K. Reduction of NO with NH_3 on Al_2O_3 and TiO_2- supported metal oxide catalysts. Ind .Eng. Chem. Res. 25 (1986): 179-186.

Yates, M., Martin, J.A., Martin-Luengo, M A., Suarez, S. and Blanco, J. N_2O formation in the ammonia oxidation and in the SCR process with V_2O_5-WO_3 catalysts. Catalysis Today 107–108 (2005): 120–125.

APPENDICES

APPENDIX A

CALIBRATING DATA FOR MASS FLOW METER

A1. Calibration data of mass flow meter are shown as follows:

Component of feed gas mixture: ammonia, nitrogen oxide, nitrogen, oxygen and sulfur dioxide

A1.1 Calibration for ammonia mass flow controller

Use the bubble flow by passing the gas through the glass tube in order to measure the time. Record the time from scale 0 ml to 5 ml of tube.

Table A1. Calibration data of ammonia mass flow controller.

Mass flow meter scale (ml/min)	**Time (sec)**			**Time average (sec)**	**Actual flow (ml/min)**
	#1	**#2**	**#3**		
1	54	54	54	54	2.22
2	24	24	24	24	5.00
3	16	16	16	16	7.50
4	12	12	12	12	10.00
5	9	9	9	9	13.33

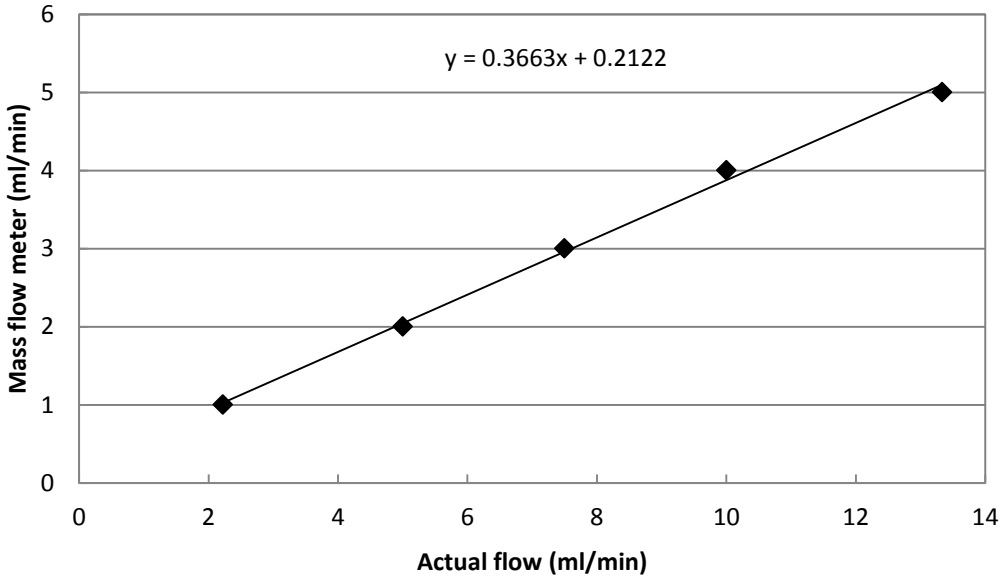

Figure A1 Calibration curve of ammonia mass flow controller.

A1.2 Calibration for nitrogen oxide mass flow controller

Use the bubble flow by passing the gas through the glass tube in order to measure the time. Record the time from scale 0 ml to 5 ml of tube.

Table A2. Calibration data of nitrogen oxide mass flow controller.

Mass flow meter (ml/min)	**Time (sec)**			**Time average (sec)**	**Actual flow (ml/min)**
	#1	**#2**	**#3**		
1	60	60	60	60	2.00
2	30	31	32	31	3.87
3	21	21	21	21	5.71
4	16	16	16	16	7.50
5	13	13	13	13	9.23

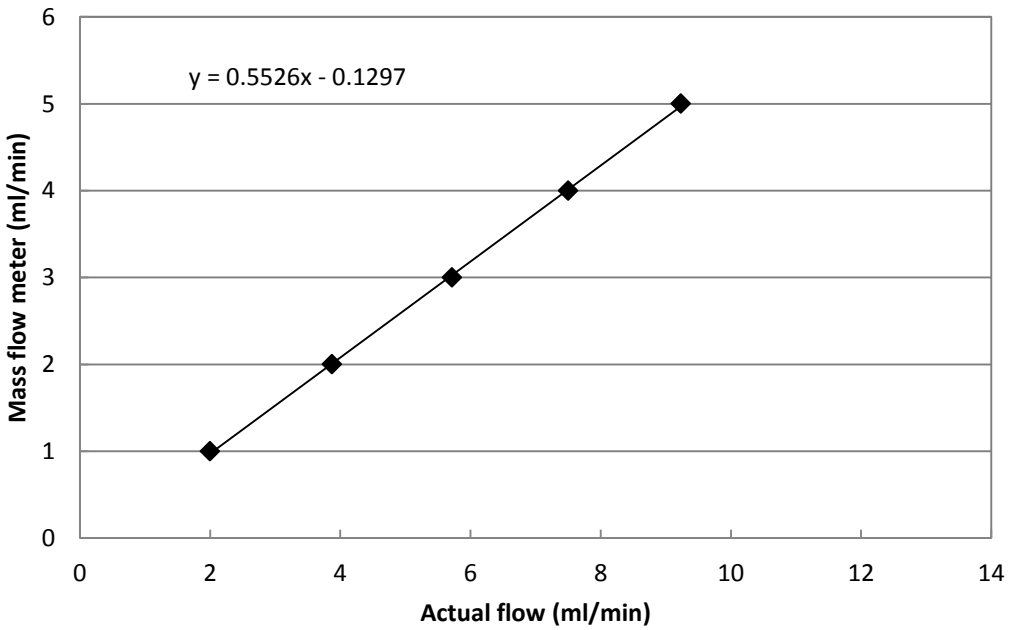

Figure A2 Calibration curve of nitrogen oxide mass flow controller.

A1.3 Calibration for oxygen mass flow controller

Use the bubble flow by passing the gas through the glass tube in order to measure the time. Record the time from scale 0 ml to 5 ml of tube.

Table A3. Calibration data of oxygen mass flow controller.

Mass flow meter (ml/min)	**Time (sec)**			**Time average (sec)**	**Actual flow (ml/min)**
	#1	**#2**	**#3**		
10	55.56	55.50	55.44	55.50	10.81
20	28.00	27.97	28.00	27.99	21.44
30	18.85	18.75	18.44	18.68	32.12
40	14.07	14.10	14.03	14.07	42.65
50	11.13	11.18	11.25	11.19	53.64

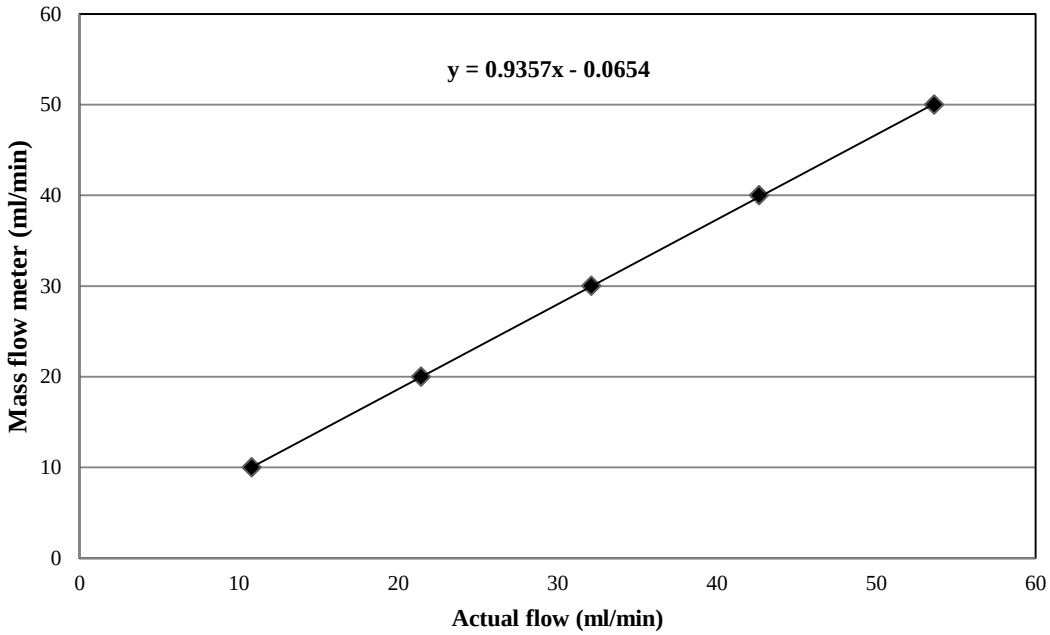

Figure A3 Calibration curve of oxygen mass flow controller.

A1.4 Calibration for nitrogen mass flow controller

Use the bubble flow by passing the gas through the glass tube in order to measure the time. Record the time from scale 0 ml to 5 ml of tube.

Table A4 Calibration data of nitrogen mass flow controller.

Mass flow meter (ml/min)	**Time (sec)**			**Time average (sec)**	**Actual flow (ml/min)**
	#1	**#2**	**#3**		
150	8	8	8	8	147
160	8	8	8	8	157
170	7	7	7	7	165
180	7	7	7	7	176
190	7	6	6	6	187

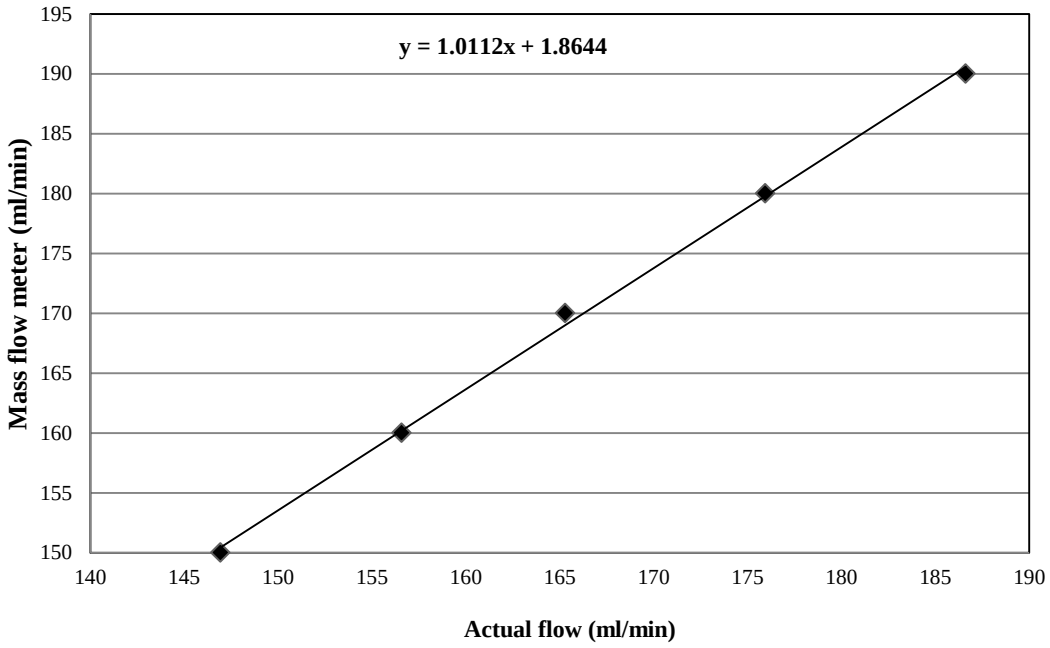

Figure A4 Calibration curve of nitrogen mass flow controller.

A1.5 Calibration for sulfur dioxide mass flow controller

Use the bubble flow by passing the gas through the glass tube in order to measure the time. Record the time from scale 0 ml to 5 ml of tube.

Table A5 Calibration data of sulfur dioxide mass flow controller.

Mass flow meter (ml/min)	**Time (sec)**			**Time average (sec)**	**Actual flow (ml/min)**
	#1	**#2**	**#3**		
1	84.9	82.5	83.59	83.66	1.43
2	38.72	38.65	39.06	38.81	3.09
3	25.34	25.50	25.31	25.38	4.73
4	18.75	18.84	18.94	18.84	6.37
5	15.32	15.43	15.37	15.37	7.81

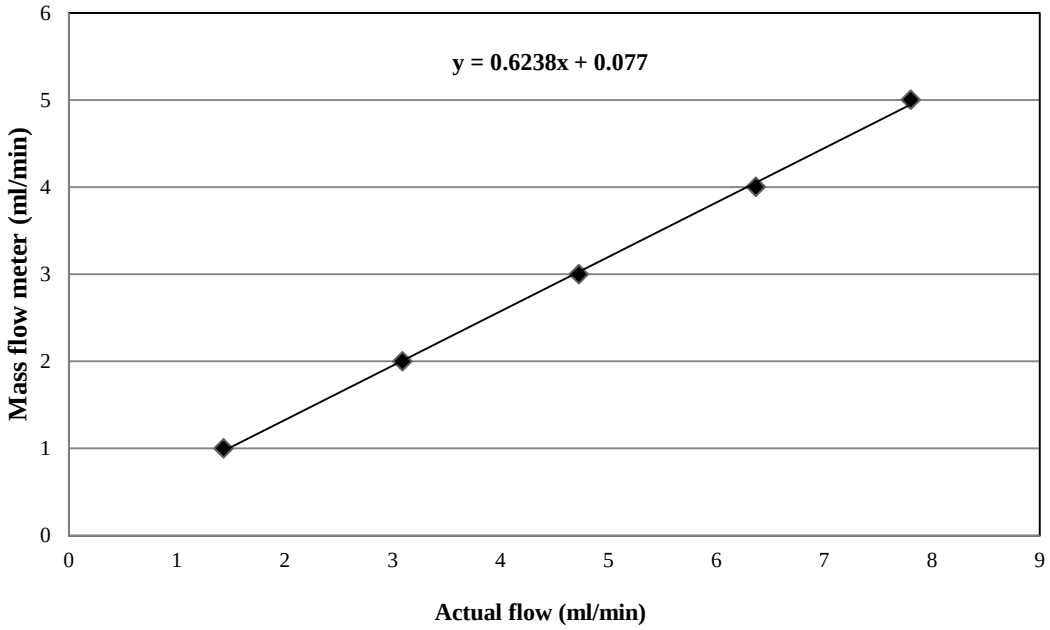

Figure A5 Calibration curve of sulfur dioxide mass flow controller.

APPENDIX B

CALCULATION FOR CATALYST PREPARATION

Preparation of V_2O_5-WO_3-MoO_3/TiO_2 catalyst is shown as follows:
Reagent:

- Titania powder prepared by a sol-gel method
- Ammonium metavanadate 99.999%
  NH_4VO_3 (Aldrich)
- Ammonium metatungsteae hydrate 99.99%
  $(NH_4)_6H_2W_{12}O_{40}•xH_{2O}$ (Aldrich)
- Ammonium heptamolybdate
  $(NH_4)_6Mo_7O_{24}•4H_2O$ (Aldrich)
- Oxalic acid hydrate (Fluka)

Calculation for the preparation of V_2O_5-WO_3-MoO_3/TiO_2

Example calculation for the preparation of 3 wt. %V_2O_5-7 wt. %WO_3-5 wt. %MoO_3
Based on 2 g of catalyst used, the composition of the catalyst will be as follows:

V_2O_5	=	0.03×2	=	0.06 g
WO_3	=	0.07×2	=	0.14 g
MoO_3	=	0.05×2	=	0.10 g
TiO_2	=	2-0.06-0.14-0.10	=	1.70 g

Vanadium oxide 0.06 g was prepared from NH_4VO_3 and molecular weight of V_2O_5 is 180.39 g/mole.

$$NH_4VO_3 \text{ required} = \frac{\text{MW of } NH_4VO_3 \times \text{vanadium oxide required} \times 2}{\text{MW of } V_2O_5}$$

$$= \frac{116.98 \times 0.06 \times 2}{180.39} = 0.0778 \text{ g}$$

Tungsten oxide 0.14 g was prepared from $(NH_4)_6H_2W_{12}O_{40}\bullet xH_2O$ and molecular weight of WO_3 is 231.84 g/mole.

$$(NH_4)_6H_2W_{12}O_{40}\cdot xH_2O = \frac{(NH_4)_6H_2W_{12}O_{40}.xH_2O \times \text{tungsten oxide required}}{12 \times MW \text{of } WO_3}$$

$$= \frac{2956.3 \times 0.14}{231.84 \times 12} = 0.1488 \text{ g}$$

Molybdenum oxide 0.10 g was prepared from $(NH_4)_6Mo_7O_{24}.\ 4H_2O$ and molecular weight of MoO_3 is 143.94 g/mole

$$(NH_4)_6Mo_7O_{24}\cdot 4H_2O = \frac{(NH_4)_2MoO_4 \times \text{molybdenum oxide required}}{7 \times MW \text{of } MoO_3}$$

$$= \frac{1235.86 \times 0.10}{7 \times 143.94} = 0.1227 \text{ g}$$

Oxalic acid require

Mole of vanadium oxide = 0.06/180.39 = 0.000333 mole

Molecular weight of oxalic acid equal to 126.07 g/mole

Oxalic acid required = 0.000333×126.07 = 0.0416 g

APPENDIX C

LIST OF PUBLICATION

บงกช ปิยานันทรักษ์, ธราธร มงคลศรี, วีรนุช กุลจรัสปกรณ์* ตัวเร่งปฏิกิริยาโลหะออกไซด์ผสม V-W-Mo บนตัวรองรับ TiO_2 สำหรับการรีดิวซ์แบบเลือกเกิดของแก๊ส NO ด้วยแก๊ส NH_3, การประชุมวิชาการวิศวกรรมเคมีและเคมีประยุกต์แห่งประเทศไทย ครั้งที่ 22, 25 – 26 ตุลาคม 2555. Ref. NO. cr-007.

VITA

Miss Weeranuch Kuljaratpakorn was born on January 03, 1989 in Chonburi, Thailand. She finished high school from Banbung Uttasahakamnukhro school, Chonburi, and graduated the bachelor's degree of Chemical Engineering, King Mongkut's Institute of Technology Ladkrabang, in 2011. She continued her master's study at Department of Chemical Engineering, Faculty of Engineering Chulalongkorn University in 2011.